International Journal on Electrical Engineering and Informatics - Volume 17, Number 4, December 2025

Optimal System Type Framework for Sustainable Energy Transition in Indonesian Isolated Microgrids: A Resource Clustering and Threshold Analysis Approach

Didik Sudarmadi[1], Iwa Garniwa[2], Budi Sudiarto[3], Muhamad Reza[4], and Suroso Isnandar[5]

[1.2.3]Department of Electrical Engineering, Universitas Indonesia, Depok, Indonesia
[4]Faculty of Electricity and Renewable Energy, Institut Teknologi PLN, Jakarta, Indonesia
[5]Directorate of Project Management and Renewable Energy, PT PLN (Persero), Jakarta, Indonesia
didik.sudarmadi@ui.ac.id, iwa@eng.ui.ac.id, budi.sudiarto@ui.ac.id,
muhamad.reza@gmail.com, suroso.isnandar@pln.co.id

Abstract: Indonesia's archipelagic geography presents unique challenges for the energy transition in isolated microgrids, where 598 installations with capacities below 1 MW predominantly operate on diesel generators, incurring significant economic and environmental costs and totaling 12 million tons of carbon emissions annually. However, existing studies predominantly address single-site hybrid renewable energy systems and do not provide a systematic, multi-location framework that links site-specific resource conditions to optimal system types (OST) and explicit energy transition pathways. This study presents a comprehensive optimal system type framework for techno-economic optimization of hybrid renewable energy systems across 130 isolated microgrid sites in Indonesia. The methodology integrates load profile clustering, renewable resource mapping, and sensitivity analysis to determine optimal configurations encompassing photovoltaic panels, wind turbines, diesel generators, battery storage, and power converters using HOMER Pro software. Load clustering analysis produced six distinct groups with strong validation metrics. At the same time, a validated generic model achieved exceptional accuracy, with a coefficient of determination of 0.985 and a Mean Absolute Percentage Error of 2.01 percent in the multi-location analysis. Case studies at four pilot sites demonstrated average Net Present Cost savings of 37.2 percent, Levelized Cost of Energy reductions of 37.1 percent, Return on Investment of 10.4 percent, and Renewable Fraction of 81.0 percent compared to diesel-only baseline systems. Beyond conventional techno-economic assessments, the proposed framework introduces a quantitative threshold analysis that identifies resource and fuel-price tipping points for technology transitions and synthesizes these findings into a multi-phase energy transition roadmap tailored to Indonesia’s national de-dieselization program. Threshold analysis identified critical transition points at a wind speed of 2.95 meters per second and Global Horizontal Irradiance levels of 5.2 and 5.5 kilowatt-hours per square meter per day for optimal technology selection. Under high-fuel-price scenarios of 1 US dollar per liter, 70.8 percent of locations achieved complete diesel elimination with pure renewable systems combining photovoltaics, wind turbines, and battery storage, while 29.2 percent retained hybrid configurations. The framework provides strategic guidance for Indonesia's national de-dieselization program targeting 5,200 diesel generator units across 2,130 locations, supporting Enhanced Nationally Determined Contribution targets and net-zero emissions by 2060.

Keywords: hybrid renewable energy system; techno-economic analysis; optimal system type; isolated microgrid; renewable energy transition; Indonesia

1. Introduction

The global energy transition represents one of the most critical sustainability challenges of the 21st century, fundamentally linking energy security, environmental protection, and social equity through the lens of sustainable development [1, 2]. Indonesia's commitment to global climate action through the Paris Agreement establishes ambitious greenhouse gas emission reduction targets of 29% through domestic efforts and 41% with international support by 2030,

Received: October 24th, 2025. Accepted: December 8th, 2025
DOI: 10.15676/ijeei.2025.17.4.3

alongside net-zero emissions by 2060 [3]. This commitment aligns directly with multiple UN Sustainable Development Goals (SSDGs, particularly SDG 7 (Affordable and Clean Energy), SDG 11 (Sustainable Cities and Communities), and SDG 13 (Climate Action), while contributing to SDG 8 (Decent Work and Economic Growth) through energy infrastructure development [4, 5]

The sustainability science literature emphasizes the importance of systems thinking and integrated approaches to address complex energy challenges [6]. The triple bottom line framework, encompassing environmental, economic, and social dimensions, provides a foundational lens for evaluating energy transition strategies [7]. In this context, isolated microgrid systems (IMS) in developing archipelagic nations such as Indonesia present unique sustainability challenges that require innovative technological and policy solutions [8].

As the world's largest archipelagic nation, comprising 17,504 islands with a 95,181 km coastline, Indonesia faces unprecedented complexities in developing an integrated electricity infrastructure that supports sustainable development goals [9]. The Indonesian Power System encompasses large-capacity networks serving major islands (Java-Bali, Sumatra, Kalimantan, and Sulawesi), ranging from hundreds of megawatts to tens of gigawatts, alongside small-capacity networks for remote islands ranging from kilowatts to tens of megawatts [10]. Currently, 157 installations operate above 1 MW, while 598 operate below 1 MW, predominantly off-grid using diesel generators (DG) [9].

The country's electricity demand is primarily met by fossil fuels, with renewable energy accounting for only 14.59% of total generation. Renewable energy includes geothermal (2.23%), hydroelectric (7.50%), biomass (3.81%), biogas (0.29%), photovoltaic (0.61%), and wind (0.15%) power generation, as shown in Fig.1. IMS predominantly relies on DGs, which introduce challenges including fuel transportation logistics, concerns about equipment reliability, maintenance requirements, and high carbon emissions totaling 12 million tons annually.

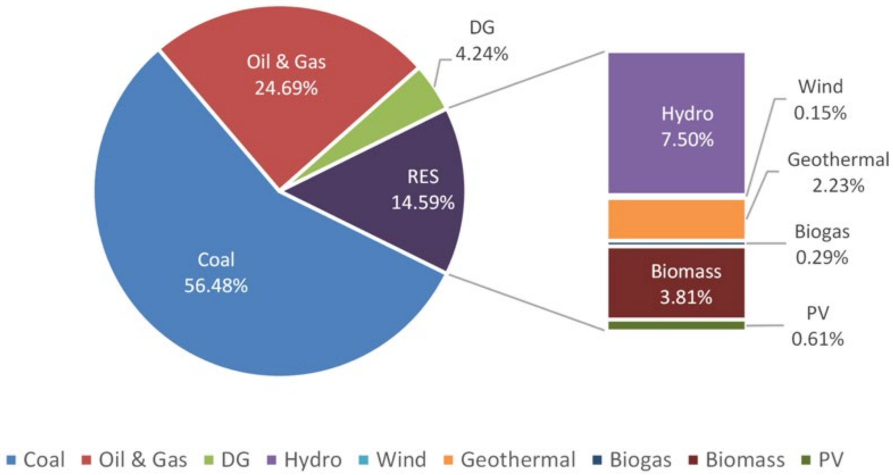

Figure 1. Installed power plant capacity by energy source (in percent) in Indonesia in 2023, with a total capacity of 85.09 GW [10].

The sustainability implications of the current energy systems are profound. IMS predominantly relies on DGs, introducing multiple sustainability challenges, including fuel transportation logistics that create economic burdens, equipment reliability concerns that affect energy security, maintenance requirements that limit local capacity development, and high carbon emissions totaling 12 million tons annually [9, 11]. In 2020, PLN managed approximately 5,200 DG units across 2,130 locations, consuming 2.7 million kiloliters of fuel annually (equivalent to IDR 16 trillion), representing significant economic and environmental costs that undermine sustainable development objectives [9].

Indonesia has substantial renewable energy potential, particularly in solar and wind resources. The nation's equatorial location provides an average Global Horizontal Irradiance (GHI) of 4.8 kWh/m²/day with remarkable year-round stability [12]. The solar potential was estimated at 207.8 GWp, with only 0.15 GWp realized by 2020 [13]. Wind resources are generally limited, with average speeds of 1.5-3.5 m/s, although certain regions exhibit higher potential suitable for hybrid system integration [14].

A. Literature Review and Research Gaps

Contemporary Hybrid Renewable Energy System (HRES) optimization employs diverse methodological approaches, ranging from metaheuristic algorithms [15] to commercial software platforms. Genetic algorithms [16] and particle swarm optimization [17] handle complex nonlinear multi-objective problems, whereas mathematical optimization techniques provide deterministic solutions [18]. Commercial platforms, particularly HOMER Pro, have emerged as industry standards for hybrid system design, offering comprehensive component libraries and integrated sensitivity analysis capabilities [19, 20].

However, current research predominantly focuses on single-location optimization [21-25], with limited systematic approaches for multi-location analysis. Studies examining multi-location contexts typically compare vastly different systems, whereas uniform-load scenarios with differential resource availability have remained underexplored. Despite these advances, most studies remain limited to single-site design or small sets of case studies, and they rarely couple multi-location techno-economic optimization with resource-based threshold analysis and explicit transition roadmaps for national-scale programs. As a result, planners still lack a systematic decision-support framework that connects local resource conditions, optimal technology choices, and phased de-dieselization pathways in archipelagic developing countries.

A systematic review of the existing literature reveals three critical gaps that this study addresses: (1) the absence of systematic OST selection frameworks relating site-specific resource variations to OST across diverse geographic contexts [22, 23]; (2) limited threshold analysis for technology transitions determining minimum resource requirements where system type transitions become economically advantageous, particularly in developing nation contexts [26, 27]; and (3) insufficient multi-location decision-support frameworks capable of automatically selecting OST across location groups based on resource indices and sustainability criteria [21, 25]. Taken together, these gaps indicate that there is no existing framework that jointly (i) optimizes hybrid renewable energy systems across many isolated microgrids, (ii) derives statistically robust resource and economic thresholds for technology switching, and (iii) translates these thresholds into operational, policy-relevant energy transition roadmaps for national de-dieselization initiatives.

B. Research Objectives and Contributions

This study addresses these critical gaps through the following key contributions to sustainability science and practice.

1. Systematic OST Framework Development: A novel methodology for the simultaneous determination of optimal HRES configurations across 130 isolated microgrid locations employing load clustering methods and comprehensive resource mapping, directly supporting SDG 7 implementation [28].
2. Validated Sustainability-Oriented Model: Development and validation of a generic techno-economic model achieving exceptional accuracy ($R^2 = 0.985$; MAPE = 2.01%) that explicitly incorporates sustainability metrics for reliable multi-location design recommendations.
3. Threshold Analysis for Sustainable Transitions: Introduction of a quantitative, statistically validated threshold analysis that determines economic and environmental breakeven conditions between various HRES configurations as functions of GHI, wind speed, and fuel price, thereby revealing explicit tipping points for technology transitions in developing nation contexts [29].

4. Multi-Location Decision Support and Transition Roadmaps: Development of OST maps and associated transition pathways for 130 isolated microgrids under multiple fuel-price scenarios, providing a scalable decision-support tool that directly informs Indonesia's national de-dieselization roadmap and can be adapted to other archipelagic systems [30].
5. Practical Implementation and Policy Integration: A comprehensive techno-economic validation across four representative case studies, combined with resource-zone classification and phased transition strategies, demonstrating how the OST framework can be operationalized by utilities and policymakers to sequence investments, prioritize high-impact sites, and design targeted policy instruments.

The remainder of this paper is organized as follows: Section 2 discusses renewable energy resources in Indonesian isolated microgrids, highlighting the potential of solar and wind resources at these sites. Section 3 focuses on the OST Framework methodology, collects meteorological and load data, applies clustering of load profiles, conducts a comprehensive techno-economic analysis of HRES and OST mapping, and concludes with threshold analysis and an energy transition roadmap. Section 4 presents the outcomes of the techno-economic optimization, maps the OST across multiple locations, identifies threshold analyses and economic tipping points, and discusses its policy implications. Section 5 presents a discussion of the results, and Section 6 concludes the paper.

2. Renewable Energy Resources in Indonesian Isolated Microgrids

A. Isolated Microgrids Characteristics

Indonesia hosts numerous IMS across small islands and remote areas. These systems serve communities with hundreds of households, predominantly residential, with typical load curves. Isolated microgrids with a capacity of less than 1 MW operate in 130 locations with a total peak load of 30.61 MW, while microgrids ranging from 1-5 MW are found in 48 locations with a combined peak load of 56.28 MW. The majority of the load was residential demand, following a typical residential load curve, as shown in Fig. 2. These microgrids are predominantly powered by DG, which are chosen for their rapid deployment, simplicity, and practicality because they do not require gas infrastructure. However, their operational costs are high, and their reliability depends heavily on fuel availability. The city is designed to accommodate the system's peak load.

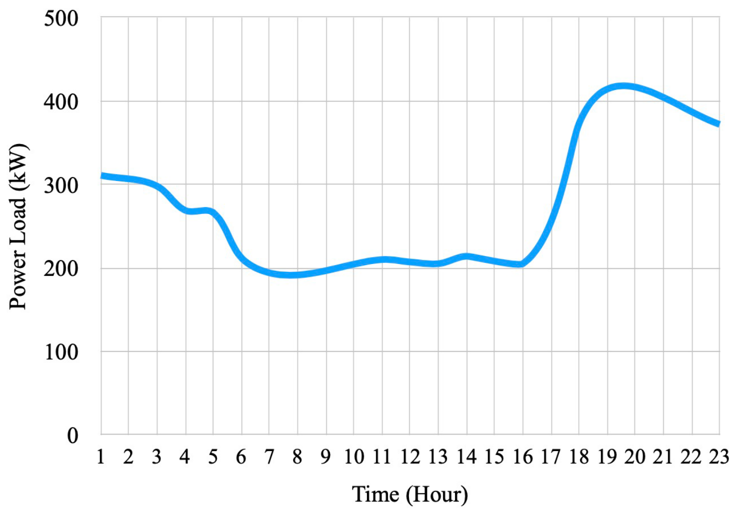

Figure 2. Load profile of the Gili Ketapang microgrid [31].

Load clustering analysis categorized these microgrids into six distinct groups based on consumption patterns, with load factors ranging from 0.664 to 0.691 and daily energy consumption spanning from 924.42 to 10,476.98 kWh/day. The clustering result is shown in Table 1, and their locations are depicted in Fig. 3.

Table 1. Hybrid Renewable Energy System Clusters.

Cluster Category	Number of Locations	Percentage	Average Energy (kWh/day)	Energy Range (kWh/day)	Average Load Factor
1	47	36.15	924.42	136 – 1925	0.664
2	42	32.31	2853.18	1951 - 3655	0.689
3	16	12.31	4534.3	3773 – 5678	0.683
4	15	11.54	6440.63	5699 - 7201	0.691
5	5	3.85	8585.6	7583 – 9580	0.668
6	5	3.85	10476.98	9898 - 11528	0.670

B. Solar Energy Potential

Indonesia's tropical location provides significant solar energy potential, with an average solar irradiation of approximately 4.8 kWh/m²/day. The monthly variation in GHI is relatively small (9-10%), and daily solar exposure typically ranges from 6 to 8 hours, depending on local meteorological conditions. A spatial representation of the average (GHI) distribution across Indonesia is shown in Fig. 4.

C. Wind Energy Potential

Indonesia faces challenges in harnessing wind energy due to relatively low wind speeds averaging 1.5-3.5 m/s. This limitation stems from Indonesia's tropical climate and its location near the equator, which results in warm air and low-pressure systems [32]. Wind across the archipelago, with some regions showing greater potential than others [33]. A spatial representation of the average wind speed distribution across Indonesia is depicted in Fig. 5.

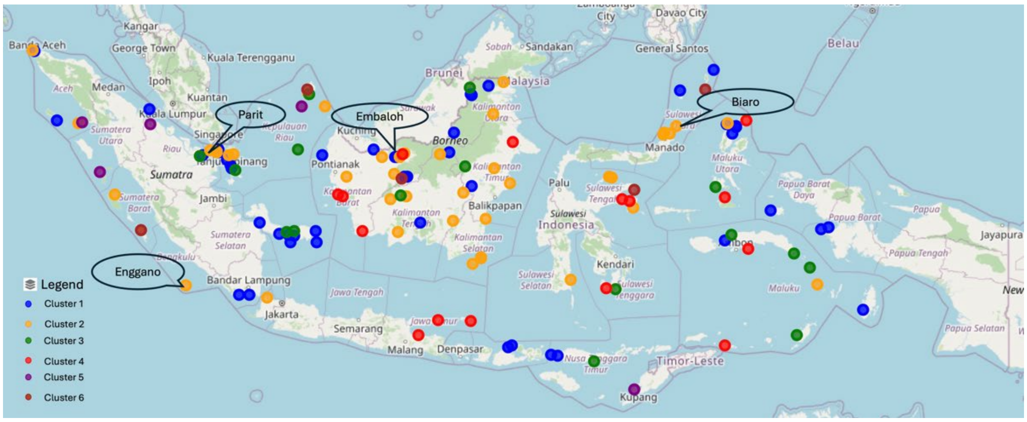

Figure 3. Location map of 130 IMS based on load clustering in 6 categories

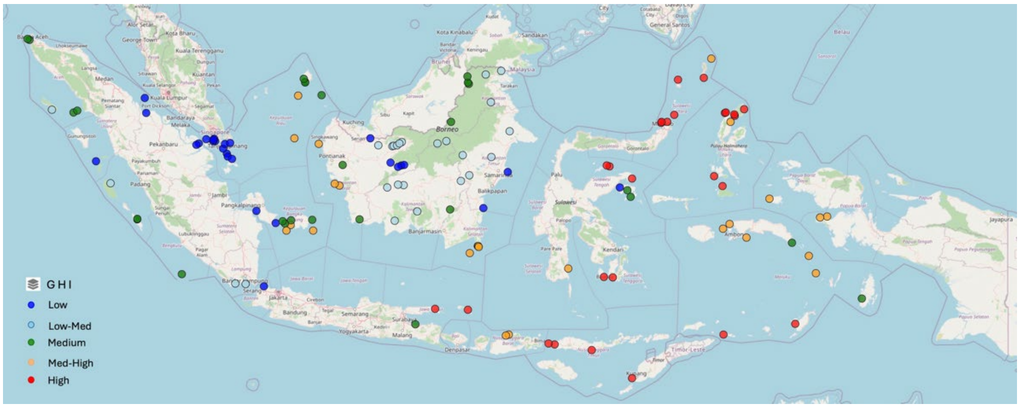

Figure 4. Map of solar energy potential in 130 IMS in Indonesia

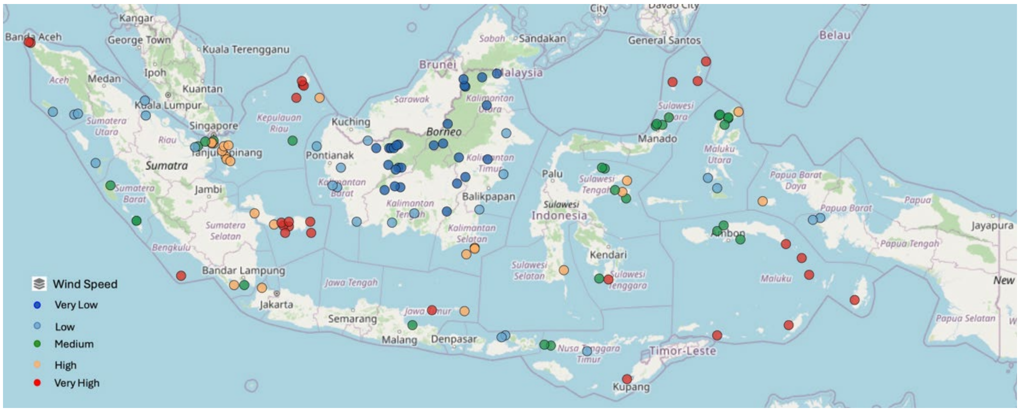

Figure 5. Map of wind energy potential in 130 IMS in Indonesia

D. Transformation Pathway

Solar and wind resources offer significant opportunities to supplement or replace existing DGs. The development of hybrid power plants integrated with existing infrastructure offers viable solutions, provided that specific technical and economic criteria are met. The declining costs of key technologies, such as solar PV, wind turbines (WT), and energy storage, continually improve the economic feasibility of renewable energy solutions [1, 34]. Fig. 6 illustrates a schematic of the transformation of an existing isolated microgrid into a hybrid renewable energy system.

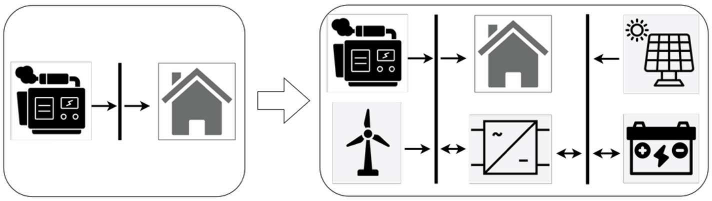
Figure 6. Transformation of diesel-powered microgrids into HRES.

3. Methodology

A. OST Framework

The OST Framework represents a novel sustainability-oriented methodology that addresses the limitations of conventional approaches in HRES optimization at the multi-location scale [35]. Unlike previous studies focusing on single-location analyses, this methodology provides a systematic approach for simultaneously determining optimal HRES configurations across 130 isolated microgrid locations in Indonesia, explicitly incorporating sustainability criteria and stakeholder considerations [36, 37]. The OST Framework comprises six integrated methodological stages that function hierarchically to deliver comprehensive multi-location renewable energy planning capabilities, as depicted schematically in Fig. 7. The six integrated methodological stages are as follows:

1. Multi-Location Data Collection and Normalization
2. Load Profile Clustering
3. Techno-Economic Analysis Modeling and HRES Optimization
4. Multi-Location OST Mapping with resource zone identification
5. Threshold Analysis Determination for Sustainable Technology Transitions
6. Energy Transition Roadmap Development

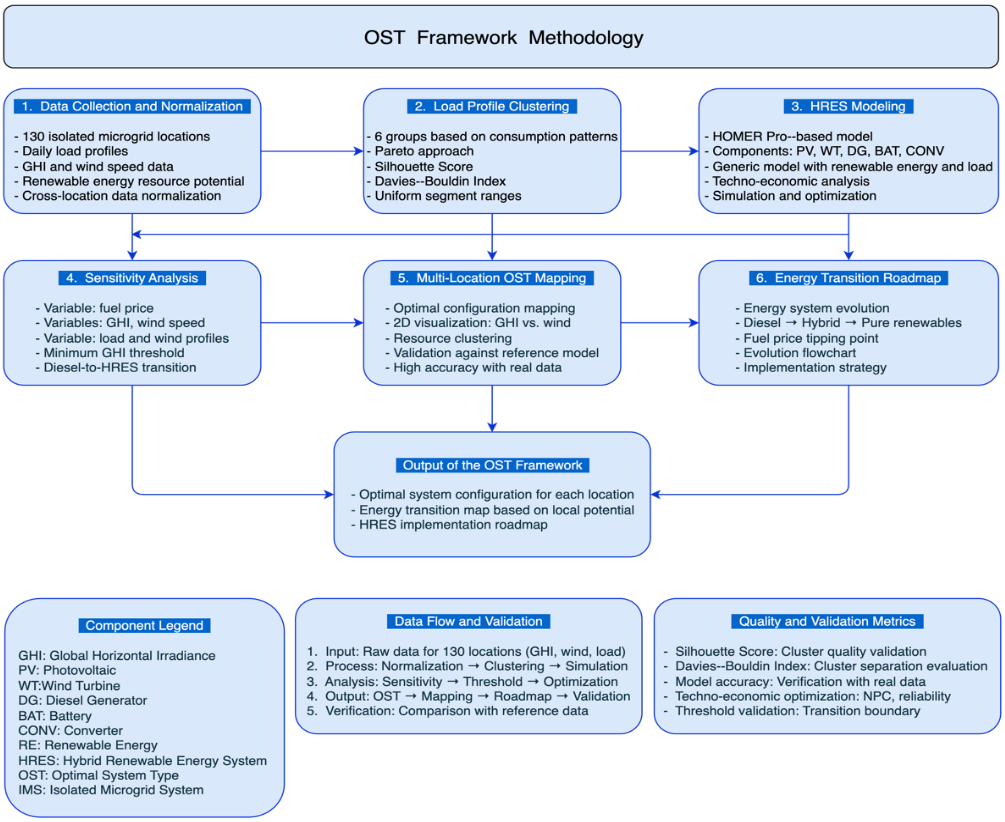

Figure 7. OST Framework Methodology

B. Data Collection and Normalization

Comprehensive data acquisition encompassed daily load profiles and meteorological resources for 130 IMS locations through systematic on-site surveys and continuous monitoring systems, ensuring data quality and representativeness for sustainability analysis [38]. Meteorological resource data, specifically GHI and wind speed measurements, were obtained from the NASA Prediction of Worldwide Energy Resources (POWER) database with a spatial resolution of 0.5° × 0.625° and multi-decade temporal coverage [39].

Data normalization procedures enabled simultaneous comparisons across diverse locations with varying scales and characteristics, facilitating accurate cross-location optimization and threshold analyses [40].

C. Load Profile Clustering

The load profile data were classified into six distinct groups using an equal-width percentile approach that reflects the empirical Pareto-like distribution of daily energy consumption across the 130 IMS. The number of six clusters was not chosen solely based on peak load, but to balance three considerations: (i) separation of systems with clearly different daily energy ranges (from 136–1,925 kWh/day up to 9,898–11,528 kWh/day as shown in Table 1), (ii) preservation of similar load factors and daily profile shapes within each cluster (typical residential evening peak patterns), and (iii) alignment with planning practice that differentiates between small (< 2 MWh/day), lower-medium (2–4 MWh/day), upper-medium (4–7 MWh/day), and large (> 7 MWh/day) microgrids. In addition to load magnitude and shape, the cluster boundaries were selected so that locations within the same cluster share comparable local renewable resource characteristics (GHI and wind speed bands, see Figs. 4 and 5), which is important for defining homogeneous "load–resource zones" for techno-economic optimization. The quality of the six-cluster solution was validated using three complementary metrics: Silhouette Score (0.57), Davies–Bouldin Index (0.51), and Calinski–Harabasz Score (611.68), demonstrating excellent clustering performance with strong cohesion within clusters and clear separation between groups.

D. Techno-Economic Analysis and HRES Optimization

1) Simulation Platform

This study employed the HOMER Pro software for a comprehensive techno-economic analysis of the proposed HRES configurations. HOMER Pro facilitates the modeling of physical characteristics. It simulates electrical energy generation from available renewable sources to meet specified load demands over defined operational lifespans, while enabling economic modeling encompassing capital expenditures, operational expenditures, and maintenance costs [19].

The simulation and optimization procedures in HOMER are shown in Fig. 8. The HRES simulation and optimization yielded the optimal system configuration, including component sizing, and a comprehensive assessment of its technical, economic, and environmental performance metrics.

The investigated HRES configurations included DG, a photovoltaic array (PV), a WT, a converter (CONV), and a battery energy storage system (BAT). These components meet the electrical load demand while leveraging solar and wind energy to supplement or replace diesel generation. A schematic of the HRES configuration is shown in Fig. 9.

2) Load Modeling

Load profiles represent the consumer electricity demand that power generation sources must meet. The load model uses annual electricity consumption represented by 8,760 hourly data points constructed from daily load profiles with significant daily variations but similar weekly trends. Typical 24-hour daily load curves recorded at each isolated microgrid location were utilized. A 5% random variability was introduced into the hourly and daily load data in the simulation to improve the forecast precision.

The load data, sourced from 130 distinct locations and defined by their average daily energy consumption (kW), were categorized into six discrete load zones. The geographical distribution of the surveyed isolated microgrid sites across Indonesia is depicted in Fig. 3, and the three-dimensional representation shown in Fig. 10 spatially correlates the variations in load profiles with the averaged GHI and wind speed. This correlation is illustrated as a load zone map to emphasize the spatial relationship between energy demand and the availability of renewable energy resources across microgrid locations.

The load profile selected for these case studies is indicative of the HRES load within load zone 2, which includes Enggano, Biaro, Parit, and Embaloh. The load data used as input for the simulations, along with the generic model employed for the sensitivity analysis, are presented in Fig. 11.

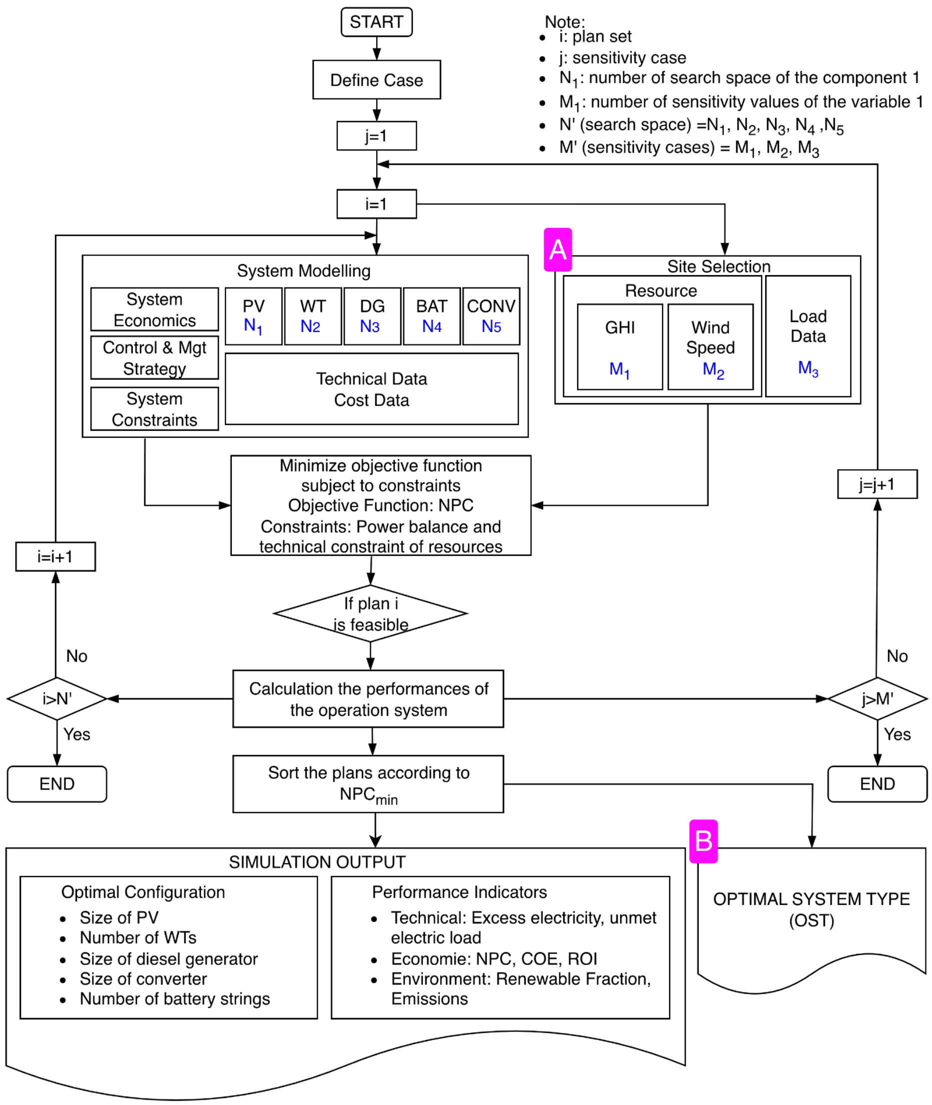

Figure 8. Flowchart of the methodology for techno-economic analysis and Homer optimization

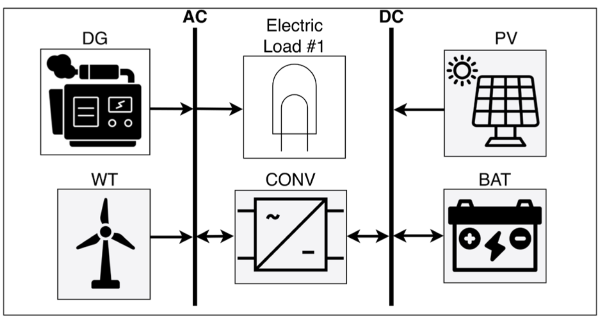

Figure 9. Schematic diagram of the studied HRES configuration.

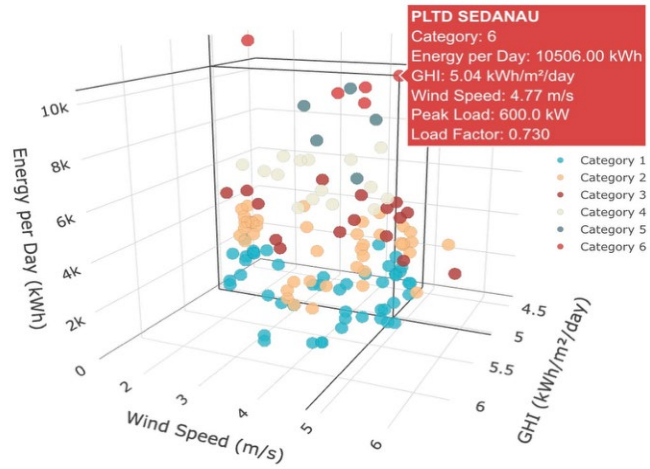

Figure 10. 3D map of GHI, wind speed, and average energy across isolated microgrids, categorized into six load zones.

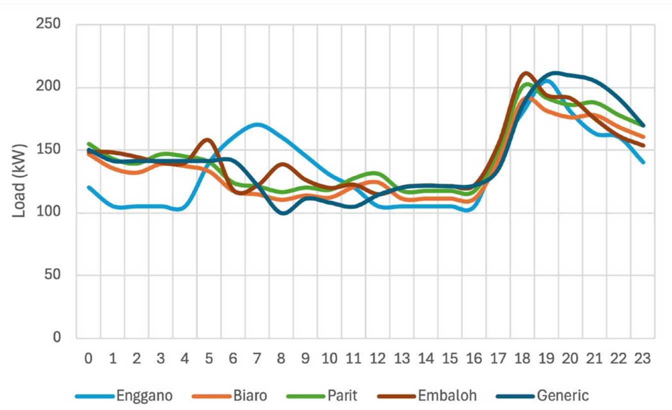

Figure 11. Daily load input in the study.

3) Components Modeling

DG denotes the current power generation infrastructure at the microgrid site. Within the HRES design, the DG functions as a dispatchable generation source, supplying additional power when renewable energy sources and the energy storage system are insufficient to meet load demand. The DG was modeled using diesel fuel as its primary energy source, with the fuel consumption model as follows [19, 41]:

$$F_{cons} = a.P_{DG} + b.P_{DG\_r} \quad (1)$$

Where P_{DG} represents the power output of the DG in kilowatts (kW) at hour t, F_{cons} is the fuel consumption in liters per hour, P_{DG_r} is the rated power output of the DG, and a and b are the fuel consumption coefficients (litres/kW).

The DG's capacity was designed to ensure it was sufficient to meet peak load demands.

The power output of a PV system is directly proportional to the incident solar irradiance, the efficiency of the PV module, and the active surface area of the PV modules, as expressed in (2) [19, 29]

$$P_{pv} = I(t) \times \eta_{pv}(t) \times A_{pv} \quad (2)$$

Where P_{pv} represents the power output of each PV module, I (kW/m^2) is the incident solar irradiance, η_{pv} denotes the PV module efficiency, and A_{pv} denotes the active surface area of the PV module.

Moreover, the PV module's efficiency is influenced by both ambient and operating temperatures. The efficiency of the PV module was calculated using the following equation [19, 29]:

$$\eta_{pv}(t) = \eta_r \times \eta_t \times [1 - \beta \times (T_a(t) - T_r) - \beta \times I(t) \times \left(\frac{NOCT-20}{800}\right) \times (1 - \eta_r \times \eta_t) \quad (3)$$

Where:

- ηr is the reference efficiency
- ηt is the efficiency of the MPPT equipment
- β is the temperature coefficient of efficiency
- Ta is the ambient temperature (°C)
- Tr is the PV cell reference temperature (°C)

The GHI data used as inputs for both the simulation and generic sensitivity models are presented in Fig. 12.

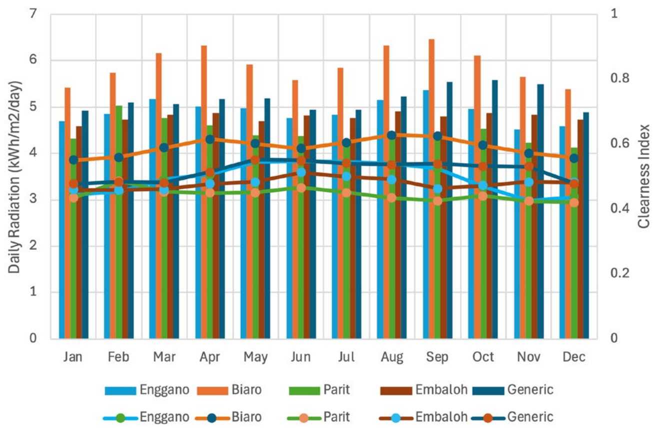

Figure 12. Daily solar radiation and clearness index data from the studied system were used.

The power output of a WT is modeled as a function of several variables, including wind direction, wind speed, air density, and height of the turbine hub. Additionally, key technical specifications, such as the generator efficiency, turbine power coefficient, and rotor-swept area, were considered. The total power output of a wind power plant is determined using equations (4) and (5) [19].

$$v(t) = v_r(t).\left(\frac{h}{h_r}\right)^{\gamma} \quad (4)$$

The wind speed v at height h is determined from the reference wind speed v_r measured at the reference height h_r using a power-law exponent γ.

$$P_W(t) = \eta_W \times \eta_g \times 0.5 \times \rho_a \times C_P \times A \times {v_r}^3 \quad (5)$$

The wind turbine power output P_W is proportional to the cube of the wind speed v, turbine efficiency η_W, generator efficiency η_g, air density ρ_a, turbine power coefficient C_P, and rotor-swept area A.

The wind speed data used as inputs for the case study and the generic wind speed profile model used in the sensitivity analysis are presented in Fig. 13. These data are essential for accurately representing wind conditions in the simulations.

Renewable energy output varies with location and weather; therefore, combining solar and wind energy in off-grid HRES improves consistency but still requires storage or backup generation. The battery size is based on the daily energy needs and desired autonomy duration, as detailed in (6) [29].

$$C_{bat} = \frac{E_l \times AD}{DOD \times \eta_{inv} \times \eta_b} \quad (6)$$

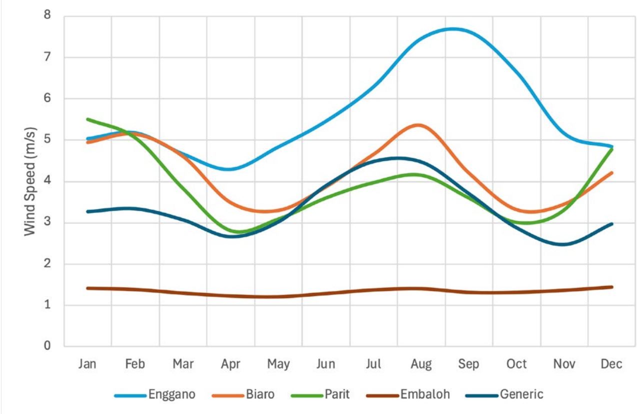

Figure 13. Input data of wind speed from the studied system

Where:

a. E_l denotes the daily load (kWh).
b. AD is the number of autonomous days.
c. DOD is the depth of discharge (80%)
d. η_{inv} and η_b are the efficiencies of the inverter and battery, respectively.

Power converters enable bidirectional conversion of electrical energy between direct current (DC) and alternating current (AC). The capacity of these converters is generally defined by the inverter's DC-to-AC conversion capacity, which specifies the maximum apparent power the inverter can deliver. In simulation scenarios, the inverter's AC power output, which fulfills the load requirements, is given by [27]:

$$P_{AC} = \eta_{inv} \times P_{DC} \quad (7)$$

where η_{inv} is the manufacturer-specified inverter efficiency, and P_{DC} is the DC power input.

4) Economic Analysis

A techno-economic evaluation of the HRES was performed to assess its cost-effectiveness over its lifetime by calculating the following key metrics: Net Present Cost (NPC), Levelized Cost of Energy (LCOE), and Return on Investment (ROI). NPC accounts for all project costs (capital, replacements, operation and maintenance (O&M), fuel, and grid electricity) minus any revenues in present value terms.

The NPC is defined as the total life-cycle cost and is calculated using the following equation [19]:

$$C_{NPC,tot} = \frac{C_{ann,tot}}{CRF(i, R_{proj})} \quad (8)$$

$$CRF(i, N) = \frac{i(1+i)^N}{(1+i)^N - 1} \quad (9)$$

where $C_{NPC,tot}$ is the total net present cost, $C_{ann,tot}$ is the total annualized cost, and CRF(i,Rproj) is the capital recovery factor, which is calculated using an annual discount rate i over the project lifetime, R_{proj}.

The LCOE is defined as the average cost per kilowatt-hour (kWh) of the net electrical energy generated and actually supplied to the load over the project lifetime, as shown in the following equation [19]:

$$LCOE = \frac{C_{ann,tot}}{E_{served}} \quad (10)$$

where E_{served} is the total electrical energy delivered to the load over the entire project lifetime (i.e., the sum of annual served energy, excluding curtailed or unmet energy).

ROI is a pivotal financial metric used to evaluate the performance of an investment by comparing the annual cost savings with the initial capital investment. The formula for this calculation is detailed in [19].

$$\mathrm{ROI} = \frac{\sum_{i=0}^{Rproj} \mathrm{Ci,ref - Ci}}{\mathrm{RProj(Ccap - Ccap,ref)}} \tag{11}$$

where $C_{i,ref}$ is the nominal annual cash flow for the reference system, C_i is the nominal annual cash flow for the current system, C_{cap} is the capital cost of the current system, $C_{cap,ref}$ is the capital cost of the reference system.

5) Technical and Economic Parameters

The component specifications and cost data for PV, WT, DG, BAT, and CONV are summarized in

Table 2, with a fuel cost of \$0.472/L reflecting subsidized pricing in Indonesia, while \$1.00/L as the market price for the sensitivity analysis.

6) Technical Constraints in the HOMER Simulations

The HRES simulations in HOMER Pro incorporated explicit technical constraints to reflect realistic operational limits for isolated microgrids. First, a maximum annual capacity shortage (unmet electricity) of 5% was imposed, consistent with the "capacity shortage" parameter in Table 2, ensuring that at least 95% of the annual load is served by the system. Second, maximum allowable excess power was constrained indirectly by limiting PV and WT capacities through economic optimization under a fixed dispatch strategy, so that the share of curtailed renewable energy remained below 10% of total potential production in all optimized configurations. Third, the minimum state of charge (SOC) for the battery bank was set to 20%, which restricted deep cycling and prevented unrealistic reliance on storage (see Table 2), while HOMER's default operating reserve and minimum load ratio settings were retained to maintain voltage and frequency stability.

In addition, the diesel generator was required to be capable of meeting the peak load plus operating reserve in all scenarios, ensuring that unmet electricity during extreme conditions was constrained by both generator sizing and the 5% capacity-shortage limit. These technical constraints jointly guarantee that the optimized HRES configurations achieve high renewable penetration without compromising supply reliability in isolated microgrids.

E. Sensitivity Analysis and OST Mapping

A sensitivity analysis was conducted to assess the impact of data uncertainty on the optimization results and sustainability metrics [19]. A sensitivity analysis evaluated the influence of key parameters — fuel cost, wind speed, solar irradiance, and load demand profiles — on the simulation outcomes. The significant outcome is the OST map, which graphically represents the least-cost system types across the ranges of the two sensitivity variables.

The OST for multiple isolated microgrids was identified using HOMER Pro's sensitivity analysis on solar irradiance, wind speed, and load profiles with a generalized HRES model, as shown in Fig. 8 (site selection box), and is detailed in Fig. 14(a).

The OST map plots average annual GHI versus wind speed for each site under a set load, overlays the resource data as scatter points, and categorizes 130 locations into six load-profile clusters. Sensitivity simulations were conducted at two distinct load levels to determine the microgrid system type within each load zone. The underlying hypothesis was that the load difference was sufficiently small, resulting in consistent system types in both simulations. To validate this assumption, the OST results were compared using the minimum and maximum load values within each load zone as inputs. The resulting microgrid system type is considered valid if its corresponding point lies within the intersection of the two OST regions. If any microgrid system fails to meet this criterion, further comparisons are necessary, iteratively narrowing the load range in subsequent simulations until all the examined systems satisfy the specified criteria.

A flowchart illustrating the validation process for OST mapping is presented in Fig. 8 (OST box) and Fig. 14(b).

Table 2. Technical and economic data of the studied HRES [19, 30, 42]

Input	Value	Input	Value
Discount rate	6,60 %	BAT	
Inflation rate	2,00 %	Quantity	1 kWh
Capacity shortage	5,00 %	Model	Lithium-ion
Project lifetime	20 year	Capital Cost	225 $
Dispatch strategy	LF	Replacement Cost	200 $
PV		O&M Cost	1.00 $/year
Capital Cost	1000 $	Lifetime	15 year
Replacement Cost	900 $	Minimum SOC	20 %
O&M Cost	10 $/year	Nominal Voltage	6 V
Lifetime	20 year	Nominal Capacity	1 kWh
Derating Factor	86 %	Maximum Capacity	167 Ah
WT		CONV	
Capital Cost	20000 $	Quantity	1 kW
Replacement Cost	15000 $	Model	Generic
O&M Cost	120 $/year	Capital Cost	600 $
Lifetime	15 year	Replacement Cost	600 $
Hub Height	16m	O&M Cost	0.02 $/year
DG		Lifetime	15 year
Model	Cummins	Efficiency	95 %
Replacement Cost	100,000 $		
O&M Cost	0.39 $/h		
Fuel Cost	0.472 $/L		
Lifetime	24,000 h		

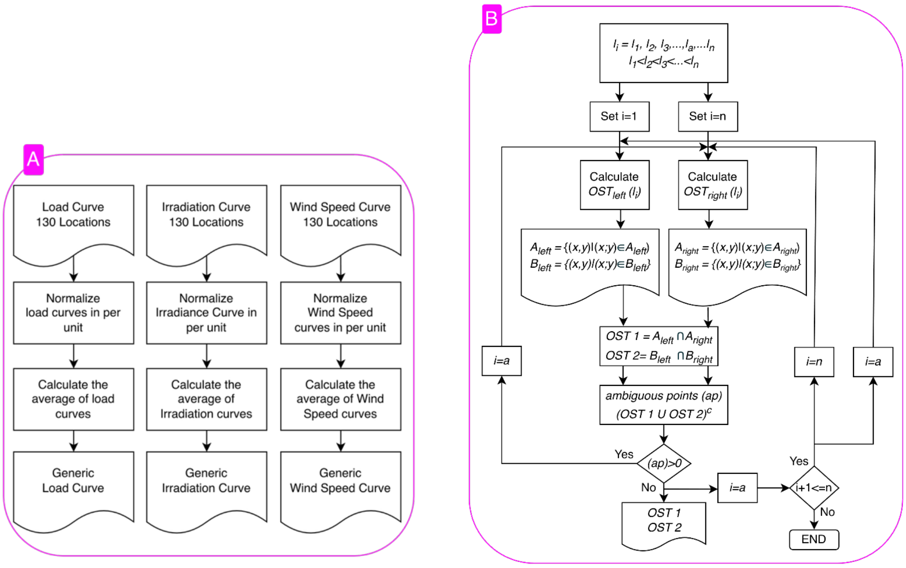

(a) (b)

Figure 14. Flowchart of (a) a generic model for OST sensitivity analysis results; (b) validation procedure to determine OST.

F. Threshold Analysis and Energy Transition Roadmap

Threshold analysis was conducted to identify the critical parameter values that trigger transitions between the optimal system configurations. Threshold analysis was conducted to identify the critical parameter values that trigger transitions between the optimal system configurations. In this study, the term “threshold” refers to resource or economic boundary values at which the least-cost optimal system type changes—for example, from DG/PV/BAT to DG/PV/WT/BAT or from diesel-backed hybrids to purely renewable PV/WT/BAT systems. This analysis integrates simulation, optimization, and sensitivity results from multi-location IMS studies to determine the threshold values for key decision variables. The candidate threshold variables were selected based on techno-economic theory and prior studies [26, 27, 41, 43, 44], namely average annual wind speed, average annual GHI, and diesel fuel price, because these directly affect the marginal cost and capacity factors of PV and WT technologies and, consequently, the comparative economics of the different OST configurations. The analysis establishes minimum wind speeds for wind turbine viability, required GHI levels for photovoltaic systems, and critical fuel prices that encourage shifts from diesel to hybrid or renewable energy systems. These thresholds help energy planners rapidly assess the potential for renewable energy deployment based on local resources and economic conditions.

The threshold analysis methodology uses statistical testing to identify transition boundaries and addresses uncertainties through Monte Carlo simulation. Practically, the workflow consists of three steps. First, for each of the 130 sites, HOMER Pro is used to obtain the least-cost OST under a wide range of wind-speed, GHI, and fuel-price combinations, using the generic HRES model described in Section 3 (Fig. 8) and the cost and technical parameters in Table 2. Second, a classification model is constructed in the (GHI, wind speed, fuel price) space to separate the regions corresponding to each OST; potential threshold values are initially identified from the empirical switching points observed in the sensitivity simulations. Third, these candidate thresholds are refined using statistical tests and Monte Carlo resampling to ensure that they maximize classification accuracy while providing narrow confidence intervals on the boundary values. This analysis provides confidence intervals for threshold values, enabling informed decision-making under uncertainty in energy planning applications [29, 41].

In the concluding phase, all prior analyses were synthesized to create detailed energy transition roadmaps. These roadmaps outline systematic progression pathways from solely diesel-based generation systems to hybrid renewable configurations and eventually to entirely renewable energy systems. They incorporate local renewable potential and fuel price scenarios, guiding the long-term development of energy infrastructure.

Transition roadmaps outline the sequence of technology deployment, accounting for capital requirements, technical complexity, maintenance, and economic returns. This approach enables coordinated energy transition planning while addressing the constraints at individual microgrid sites.

The system evolution flowcharts show decision points and transition criteria, guiding implementation timing and technology selection under various economic and resource conditions. In summary, the threshold analysis provides the quantitative backbone of the energy transition roadmap: each phase of the roadmap (Section “Policy Implications and Strategic Guidance”) is defined by the progression across these resource and fuel-price thresholds, ensuring that the recommended sequence of technology deployment is consistent with both least-cost optimization results and statistically robust tipping points. These roadmaps support project development and policy formulation for sustainable energy transition in microgrids.

G. Statistical Analysis and Model Validation

The study employed a sample of 130 locations, providing 95% statistical power to detect medium effect sizes (Cohen's d = 0.5) in renewable energy performance comparisons across different system configurations, assuming $\alpha = 0.05$ [45]. This sample size is adequate for robust statistical inference and generalization to the broader population of Indonesian isolated microgrids [46]

Model validation testing was conducted by calculating key evaluation metrics —Mean Absolute Error (MAE), Mean Squared Error (MSE), Root Mean Squared Error (RMSE), and Coefficient of Determination (R^2) — across 30 cases, comparing the generic model to the detailed model. The validation results were as follows: MSE: 0.003463, RMSE: 0.058850, MAE: 0.048333, and MAPE: 2.014529%. All four metrics consistently demonstrated high accuracy, indicating a robust model performance suitable for policy-relevant analysis.

In this context, each statistical parameter serves a distinct role in evaluating the robustness of the proposed framework. The Mean Absolute Error (MAE) and Mean Squared Error (MSE) quantify the magnitude of absolute and squared deviations between the generic and detailed models, with low values indicating that the simplified generic model can reliably reproduce location-specific techno-economic outputs. The Root Mean Squared Error (RMSE) provides an interpretable error metric in the same units as the response variable, facilitating comparison with practical planning tolerances. The Coefficient of Determination ($R^2 = 0.985$) measures how much of the variance in detailed-model outputs is explained by the generic model, which is critical for justifying the use of a single generic configuration across multiple sites. The Mean Absolute Percentage Error (MAPE ≈ 2.0%) expresses errors in relative terms and confirms that the model remains accurate across locations with different load and resource levels. Finally, the statistical power analysis (95% at $\alpha = 0.05$ for 130 locations) ensures that the sample size is sufficient to detect meaningful differences in system performance between configurations and resource zones, thereby supporting the generalizability of the findings to the broader IMS population.

The Monte Carlo simulation employed 78,000 iterations across 130 microgrid sites to establish the statistical robustness of the threshold analysis [47]. Scenario 1 (S1) classification accuracy reached 99.2% under baseline fuel prices (USD 0.472/L), whereas Scenario 2 (S2) accuracy was 45.4% at elevated prices (USD 1.00/L), yielding an overall accuracy of 72.3%. The critical wind speed (2.95 m/s) and GHI (5.2 and 5.5 kWh/m²/day) thresholds were validated with narrow 95% confidence intervals (±0.08–0.06 for GHI; ±0.08 for wind speed) and coefficients of variation below 3.5%. Convergence was achieved after approximately 50,000 iterations. Sensitivity analysis showed ±10% variations in wind and solar inputs shifted thresholds by ±0.15 m/s and ±0.25 kWh/m²/day, respectively, while ±20% changes in component costs shifted thresholds by ±0.35 m/s and ±0.40 kWh/m²/day. Uncertainty propagation maintained 95% prediction intervals covering 94.7% of observed outcomes, and spatial validation (Pearson $r = 0.847$, $p < 0.001$; Moran's $I = 0.312$, $p < 0.01$) confirmed regional representativeness, with the High Resource and Ultimate Pure Renewable zones achieving 96.7% and 100% classification accuracy, respectively.

4. Results

A. Techno-Economic Optimization Results

1) Economic Performance Analysis

Optimizing HRES yields substantial economic gains relative to the diesel-only baseline across all four locations, as shown in Table 3. This finding aligns with recent research on the economic viability of renewable energy in Indonesia [11, 48, 49]. It shows substantial cost reductions and improved economic indicators aligned with international renewable energy project performance [22, 26, 50].

The implementation of optimal HRES systems demonstrated significant economic advantages compared to diesel-only baseline scenarios across all four case study locations. NPC savings ranged from 27.9% to 50.0%, with an average of 37.2%. Enggano achieves the most significant savings, with NPC decreasing from USD 3.88 million to USD 1.94 million, representing a savings of USD 1.94 million (50.0%).

Table 3. Optimization Results of the Studied HRES.

Location	Case	PV (kW)	WT (Qty)	DG (kW)	BAT (kW)	CONV (kW)	NPC (M$)	LCOE ($/kWh)	ROI (%)	RF (%)
Enggano	Optimum	338	19	600	1664	201	1.94	0.125	15.1	84.6
	Based	-	-	600	-	-	3.88	0.250	-	-
Biaro	Optimum	583	13	600	2886	216	2.23	0.143	10.6	91.0
	Based	-	-	600	-	-	3.86	0.248	-	-
Parit	Optimum	574	17	600	2091	200	2.78	0.172	8.4	71.3
	Based	-	-	600	-	-	3.9	0.240	-	-
Embaloh	Optimum	873	-	600	3114	238	2.81	0.171	7.6	77.2
	Based	-	-	600	-	-	3.9	0.237	-	-

The average LCOE reduction was 37.1%, with Enggano leading at a 50% reduction from USD 0.250/kWh to USD 0.125/kWh. These values are broadly consistent with, and in several cases more favorable than, techno-economic results reported for comparable hybrid PV–diesel or PV–wind–diesel systems in other developing contexts. For example, [22] reported LCOE reductions of 25–35% for hybrid microgrids in Bangladesh, while [27] and [26] obtained 20–40% reductions and ROIs in the range of 5–9% for North African and Indian case studies, respectively. ROI analysis reveals attractive investment prospects, with Enggano demonstrating the highest ROI at 15.1%, followed by Biaro (10.6%), Parit (8.4%), and Embaloh (7.6%). The average ROI of 10.4% substantially exceeds the typical returns from renewable energy projects reported in the literature for remote microgrids, which commonly range between 5–9% [22, 26, 27, 51]. This indicates that, under the Indonesian cost and resource conditions considered here, HRES investments are not only viable but also competitive with conventional infrastructure investments from a utility or private investor perspective.

Fig. 15 presents a normalized radar chart for the multi-criteria performance comparison of the NPC, LCOE, ROI, and RF. Enggano attained the highest ranking (score 100) with optimal performance in NPC, LCOE, and ROI. In contrast, Biaro secured second place with excellent RF performance (91.0%), demonstrating the effectiveness of high solar resource utilization.

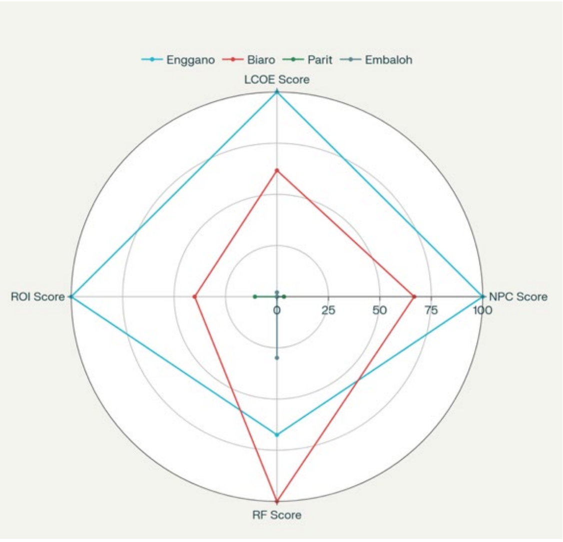

Figure 15. Normalized Radar Chart for Multi-Criteria Performance Comparison of HRES at Four Locations

2) Electrical Performance and Energy Production

The monthly energy production profiles, shown in Fig. 16, demonstrate renewable energy dominance across all configurations, with seasonal variations consistent with Indonesia's tropical climate. PV generation is the primary energy source in Embaloh (80.9%), Biaro (69.3%), and Parit (51.1%), whereas WT dominates in Enggano (56.0%) owing to superior coastal wind resources.

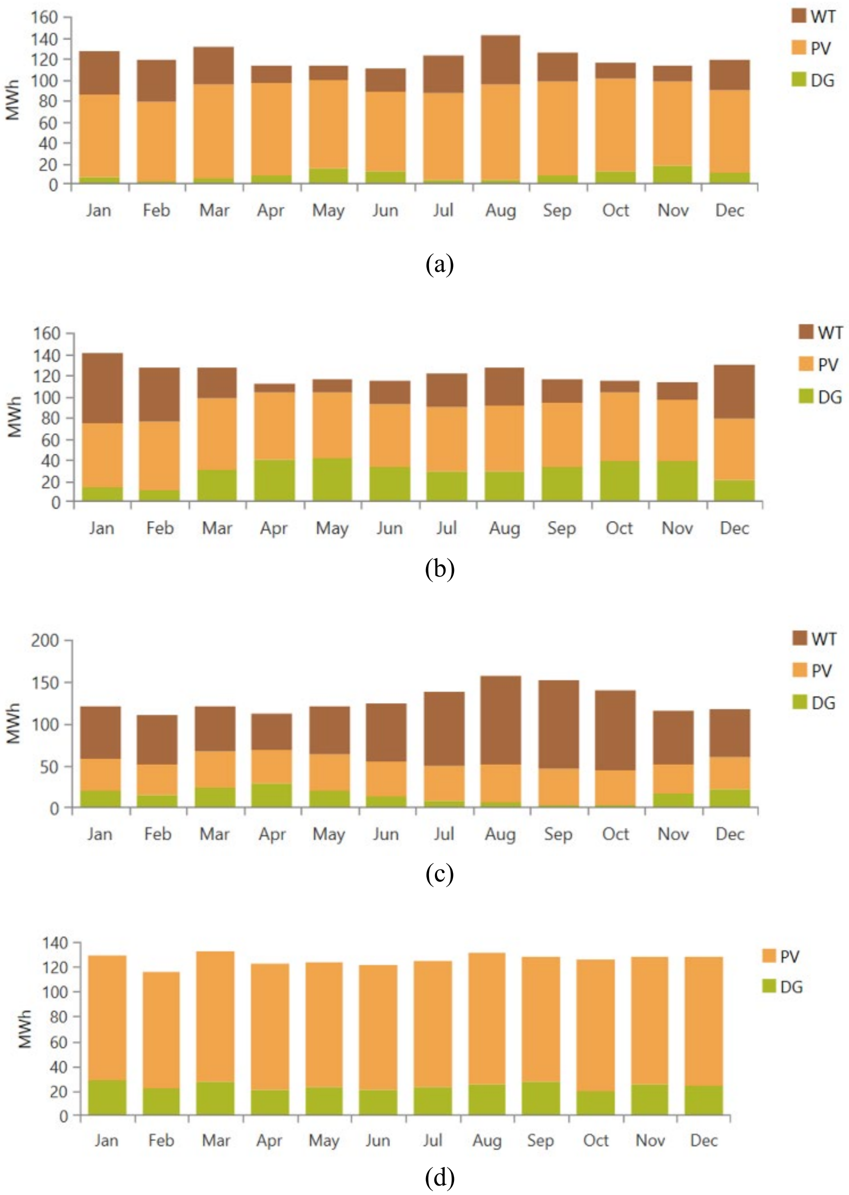

Figure 16. Monthly Electrical Energy Production for (a) Biaro, (b) Parit, (c) Enggano, and (d) Embaloh.

Table 4 presents the quantified annual contributions of various components, confirming the substantial integration of renewable energy sources. In Embaloh, PV systems accounted for 80.9% of the total annual energy production of 1,507 MWh. In Biaro, PV systems accounted for 69.3% of the 1,451 MWh total, whereas in Parit, they accounted for 51.1% of the 1,458 MWh total. Enggano benefits from a superior wind regime, resulting in WT contributing 56.0% of the total 1,527 MWh. DGs contributed less than 25% at all locations, ranging from 7.4% in Biaro to 24.5% in Parit, serving primarily as backups to enhance reliability and manage operational costs.

3) Environmental Sustainability Performance

The contribution of renewable energy exceeded 70% across all sites, reaching 91% in Biaro, indicating a significant displacement of fossil fuels in line with the national renewable energy objectives. The capacity factors further demonstrate the efficient utilization of resources: PV systems exhibit operational ranges of 14.8-19.7%, typical of equatorial regions, whereas DG units operate at minimal levels of 2.1–6.8%, underscoring their role as emergency backups.

The transition to optimized HRES configurations yields substantial environmental benefits, including quantified reductions in carbon emissions [52].

- Average CO_2 emission reduction: 78.3% compared to diesel-only systems
- Total annual emission reduction across four sites: 2,847 tons CO_2/year
- Equivalent to removing 619 passenger vehicles from roads annually
- Carbon benefit valuation: USD 142,350/year at USD 50/tCO_2

Table 4. Electrical Energy Production

Location	**Enggano**		**Biaro**		**Parit**		**Embaloh**	
ID	**z2_33**		**z2_34**		**z2_35**		**z2_37**	
Components	**MWh/yr**	**%**	**MWh/yr**	**%**	**MWh/yr**	**%**	**MWh/yr**	**%**
PV	487	32	1005	69	745	51	1219	81
DG	184	12	108	7.5	358	25	288	19
WT	856	56	338	23.5	355	24	-	-
Total	1527	100	1451	100	1458	100	1507	100

B. OST Mapping and Multi-Location Analysis

1) OST Mapping Results

The OST simulation was conducted at 130 microgrid sites, divided into six distinct load zones. The simulations were based on two different fuel cost scenarios: Scenario 1 (OST1), with a fuel price of $0.472 per liter, and Scenario 2 (OST2), with a fuel price of $1.00 per liter. Each scenario produced eight OST map-image pairs. Due to limited space in this article, only one representative image from each scenario is displayed, as shown in Fig. 17 and summarized in Table 5.

A comprehensive OST analysis across 130 microgrid sites revealed distinct resource zones that inform strategic planning for renewable energy deployment [53]. In Scenario 1, the configurations predominantly fell into two categories: green (DG/PV/WT/BAT), representing 69.2% (90 locations), and red (DG/PV/BAT), representing 30.8% (40 locations). PV systems consistently emerge as essential HRES components, whereas WT becomes uneconomical below an average wind speed of approximately 3 m/s.

Scenario 2 demonstrated a radical transformation with four configuration types: blue (PV/WT/BAT) at 58.5% (76 locations), yellow (PV/BAT) at 12.3% (16 locations), green at 9.2% (12 locations), and red at 20.0% (26 locations). Notably, 70.8% of the locations achieved complete diesel elimination at a fuel price of $1.00 per liter.

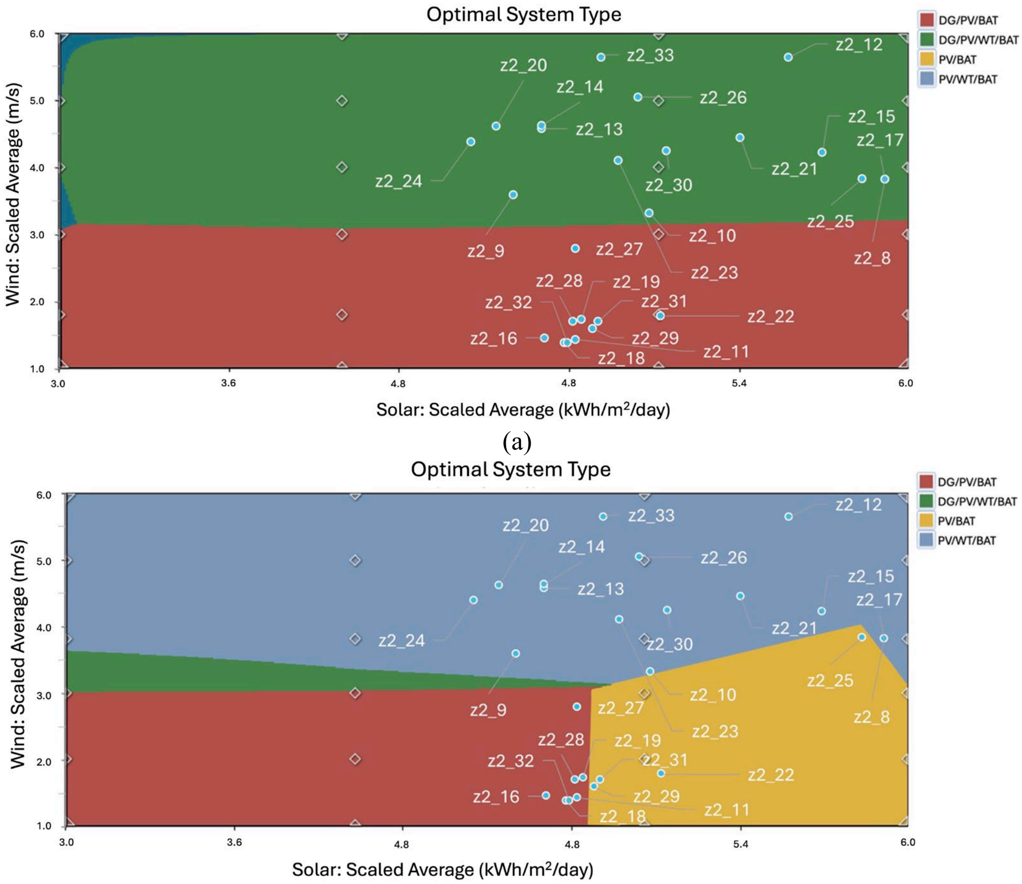

(a)

(b)

Figure 17. OST Map (a) Scenario 1 z2_8-z2_33, (b) Scenario 2 z2_8-z2_33

A comparative OST mapping across 130 locations in Indonesia revealed distinct configuration transitions between the two scenarios, as depicted in Fig. 18. This figure illustrates the geographical distribution of microgrid sites across Indonesia, with each site encoded by its classification under the OST1 and OST2 configurations. The left half of each bicolored marker represents OST1, and the right half represents OST2.

Under the OST1 scenario, the spatial distribution shows three main renewable energy zones. The western regions of Sumatra and Java demonstrated moderate potential, with yellow markers for PV/BAT systems and scattered green dual-qualified PV/WT/BAT sites. The central regions, including Sulawesi and Maluku, showed limited feasibility with red DG/PV/BAT markers. Northern Sulawesi and eastern Kalimantan emerged as high-resource zones, with green markers indicating viable PV and WT technologies.

The transformation of the OST2 scenario revealed notable threshold sensitivity across all regional clusters. In the western region of Indonesia, the transition indicated a moderate enhancement, with approximately 30-40% of yellow OST1 sites advancing to a green dual-qualified status. This suggests that reductions in technology costs or improvements in component efficiency could facilitate the integration of WT in locations previously designated for solar energy only. The central and eastern archipelagic regions exhibited the most pronounced transformation, characterized by significant red-to-yellow transitions. These transitions represent sites where relaxed economic constraints permit the deployment of PV/BAT systems, thereby reducing diesel dependency from a primary to a backup-only configuration.

Table 5. OST Map Scenario 1 and Scenario 2 for ID z2_8-z2_33

No	Name	ID	Energy Perday (kWh/day)	GHI (kWh/m2/ day)	Wind Speed (m/s)	OST1[1]	OST2[1]
55	PLTD Mantehage	z2_8	2418	5.91	3.82	2	4
56	PLTD Muara Pantuan	z2_9	2531	4.6	3.59	2	4
57	PLTD Haloban	z2_10	2542	5.08	3.32	2	4
58	PLTD Long Peso	z2_11	2578	4.82	1.44	1	1
59	PLTD Kur	z2_12	2590	5.57	5.63	2	4
60	PLTD Karas	z2_13	2590	4.7	4.57	2	4
61	PLTD Mantang	z2_14	2590	4.7	4.62	2	4
62	PLTD Gangga	z2_15	2590	5.69	4.22	2	4
63	PLTD Tebidah	z2_16	2659	4.71	1.46	1	1
64	PLTD Nain	z2_17	2763	5.91	3.82	2	4
65	PLTD Long Apari	z2_18	2786	4.78	1.39	1	1
66	PLTD Tumbang Manjul	z2_19	2818	4.84	1.74	1	1
67	PLTD Pulau Panjang	z2_20	2847	4.54	4.61	2	4
68	PLTD Marabatuan	z2_21	2861	5.4	4.44	2	4
69	PLTD Pulau Limbung	z2_22	2880	5.12	1.79	1	3
70	PLTD Seay Baru	z2_23	2881	4.97	4.1	2	4
71	PLTD Pulau Terong	z2_24	2888	4.45	4.38	2	4
72	PLTD Dolong	z2_25	2938	5.83	3.83	2	3
73	PLTD Tanjung Kumbik	z2_26	2972	5.04	5.04	2	4
74	PLTD Telaga Pulang	z2_27	3043	4.82	2.79	1	1
75	PLTD Tumbang Hiran	z2_28	3049	4.81	1.71	1	1
76	PLTD Sedulang	z2_29	3053	4.88	1.6	1	3
77	PLTD Lipulalongo	z2_30	3056	5.14	4.24	2	4
78	PLTD Sei Menggaris	z2_31	3110	4.9	1.71	1	3
79	PLTD Ujung Said	z2_32	3126	4.79	1.39	1	1
80	PLTD Enggano	z2_33	3268	4.91	5.63	2	4

[1] Optimal System Type (OST) codes and legend: 1 (red): DG/PV/BAT; 2 (green): DG/PV/WT/BAT;
3 (yellow): PV/BAT; 4 (blue): PV/WT/BAT

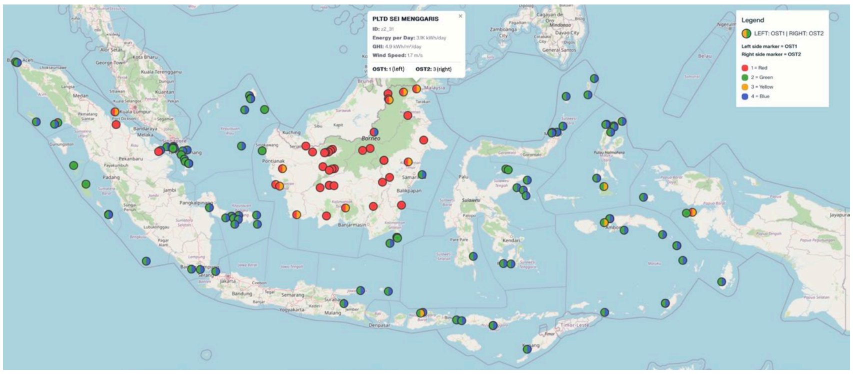

Figure 18. OST map at 130 locations in six load clusters for Scenarios 1 and 2.

In the northern high-resource zones, the green dual-qualified status is maintained under both scenarios, with geographical expansion that includes additional sites achieving PV/WT/BAT feasibility. The example of PLTD Sei Menggaris (GHI = 5.7 kWh/m²/day, wind = 5.7 m/s) illustrates locations where OST2 conditions facilitate the complete elimination of diesel, transitioning from DG/PV/BAT to purely renewable PV/WT/BAT configurations.

The transition from OST1 to OST2 reveals distinct pathways for technology adoption, influenced by the characteristics of the available resources. Sites with marginal wind resources (3-4 m/s) showed marked sensitivity to changes in economic thresholds, shifting from PV-only systems to hybrid PV and WT configurations under OST2 conditions. In areas with moderate solar resources and insufficient wind resources, the feasibility of PV and BAT systems is enhanced by reducing component costs or improving system efficiency. Locations with abundant resources achieve full renewable energy potential under OST2, aligning with Indonesia's strategic goals for deploying advanced hybrid systems.

The spatial analysis substantiates that Indonesia's renewable energy potential far exceeds the current economic thresholds. OST2 scenarios demonstrate the adaptability of pathways to meet national renewable energy targets by optimizing costs through technology and deployment strategies tailored to regional conditions.

2) Energy Resource Transformation Pathways

Fig. 19 depicts the compositional transformation between Scenarios 1 and 2. The composition transformation between scenarios revealed a 70.8 percentage-point reduction in diesel dependency. The dominant transition pattern shifted from green (DG/PV/WT/BAT) to blue (PV/WT/BAT), with 75 locations (57.7%) following this radical transformation pathway [54].

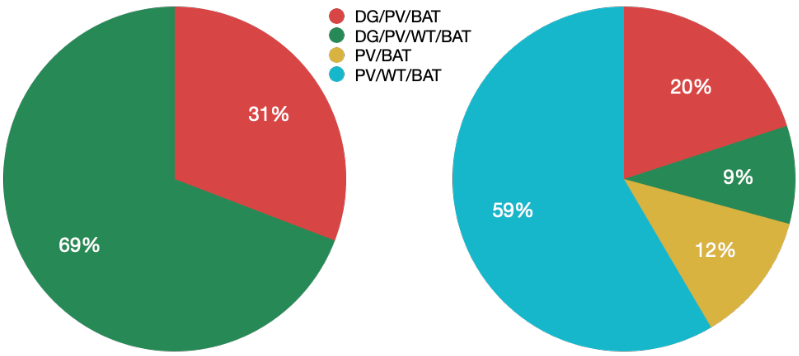

Figure 19. Composition of OST in Scenario 1 and Scenario 2

Table 6 presents a classification of six distinct transition pathways defined by the progression of renewable fractions and alterations in system complexity. Fig. 20 shows the pathway transition from the existing condition toward the transition paths for Scenarios 1 and 2. Conservative pathways, characterized by an RF of 30-50%, involve transitions from DG/PV/BAT to DG/PV/BAT and affect 26 locations (20.0%). These pathways indicate sites with minimal resource enhancement under optimized conditions. In contrast, moderate pathways, with an RF of 85-95%, included transitions from DG/PV/BAT to PV/BAT (12 locations, 9.2%) and from DG/PV/WT/BAT to PV/BAT (4 locations, 3.1%), reflecting the removal of diesel through improved storage integration.

Radical pathways, characterized by a 90-100% renewable fraction (RF), predominate the transformation landscape. The transition from DG/PV/WT/BAT to PV/WT/BAT constituted the primary route, impacting 75 locations, which accounted for 57.7% of the total sites. This pathway illustrates the economic feasibility of wind-solar hybrid systems under optimized fuel price scenarios, where wind turbine capacity factors of 25-35% and PV capacity factors of 18-22% achieve competitive economics under Indonesian conditions. Additionally, the DG/PV/BAT-to-

PV/WT/BAT pathway affected 1 location (0.8%), representing sites where optimizing wind resources enabled the complete elimination of diesel use.

Table 6. Renewable Fraction Transformation Paths [51, 55-57].

Transition Path	Location	Percentage	Evolution Type	RF (%)
DG/PV/BAT → DG/PV/BAT	26	20.0	Conservative	30-50
DG/PV/BAT → PV/BAT	12	9.2	Moderate	85-95
DG/PV/BAT → PV/WT/BAT	1	0.8	Radical	90-100
DG/PV/WT/BAT → DG/PV/WT/BAT	11	8.5	Conservative	50-70
DG/PV/WT/BAT → PV/BAT	4	3.1	Moderate	85-95
DG/PV/WT/BAT → PV/WT/BAT	75	57.7	Radical	90-100

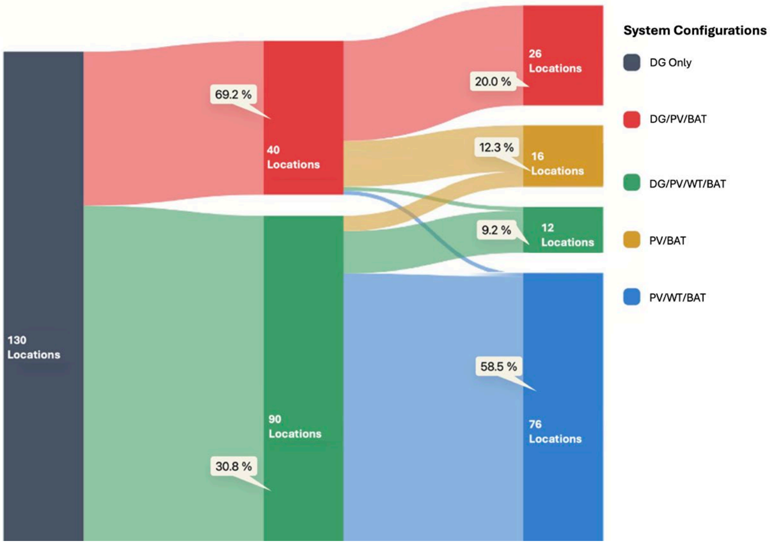

Figure 20. Sankey diagram of system configuration evolution for 130 Indonesian IMS from Diesel Only to HRES

C. Threshold Analysis and Economic Tipping Points

Critical threshold analysis identifies the breakeven points for wind speed and GHI, which guide optimal technology choices for sustainable energy transitions [43]. A detailed Monte Carlo simulation comprising 78,000 iterations across 130 sites, as illustrated in Fig. 21, yielded classification accuracies of 99.2% and 45.4% for Scenarios 1 (S1) and 2 (S2), respectively, culminating in an overall accuracy of 72.3% [44].

In scenario S1, a wind speed threshold of 2.95 m/s effectively distinguished between the DG/PV/BAT and DG/PV/WT/BAT configurations, suggesting that even slight increases in average wind speed warrant integrating turbines at baseline fuel prices. In the higher-cost scenario S2, two elevated wind thresholds at 4.0 m/s and 4.5 m/s further delineate the feasibility of purely renewable configurations and indicate the transition from PV/BAT to PV/WT/BAT dominance as fuel prices escalate.

Concurrent GHI breakeven points at 5.2 and 5.5 kWh/m²/day delineate progressive zones of solar viability. Locations with GHI values exceeding 5.2 kWh/m²/day are suitable for photovoltaic and battery (PV/BAT) systems. In contrast, those surpassing 5.5 kWh/m²/day enter the Ultimate Pure Renewable Zone, achieving full deployment of photovoltaic, wind turbine, and battery (PV/WT/BAT) systems under Scenario 2 (S2).

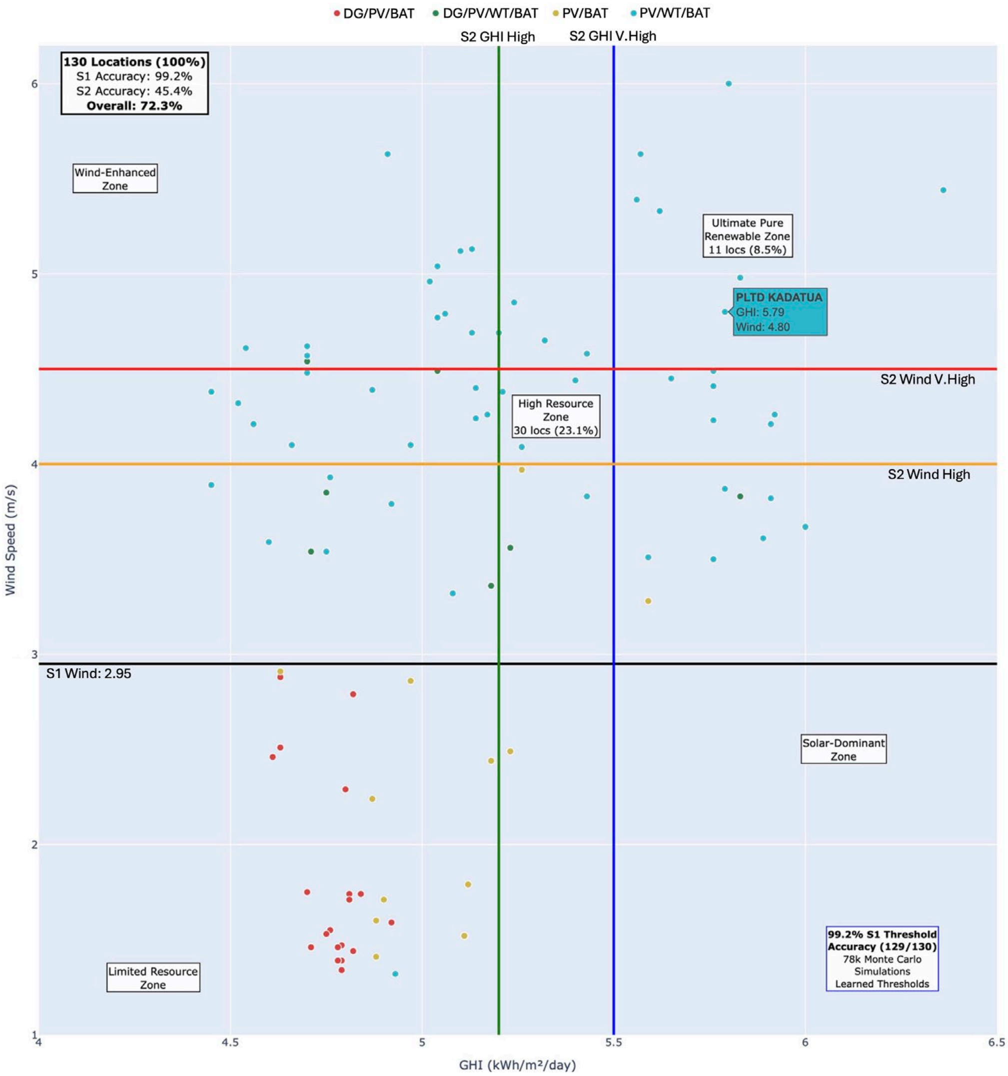

Figure 21. GHI vs Wind Speed Threshold Analysis for 130 IMS

The classification of these thresholds delineated five distinct resource zones. The Limited Resource Zone, identified by a GHI of less than 4.5 kWh/m²/day and wind speeds under 2.95 m/s, continues to rely on diesel. The Wind-Enhanced Zone, characterized by wind speeds greater than 2.95 m/s and GHI below 5.2 kWh/m²/day, facilitates the integration of DG, PV, WT, and BAT in Scenario 1 (S1) and the transition to PV, WT, and BAT in Scenario 2 (S2). The Solar-Dominant Zone, with GHI values exceeding 5.5 kWh/m²/day and wind speeds under 4.0 m/s, supports the deployment of PV and BAT in S2. The High Resource Zone, where GHI is at least 5.2 kWh/m²/day and wind speeds are at least 4.0, includes 30 locations, accounting for 23.1% of the total, with a 96.7% adoption rate of PV, WT, and BAT. The Ultimate Pure Renewable Zone, defined by GHI values of 5.5 kWh/m²/day or higher and wind speeds of 4.5 m/s or higher, comprises 11 locations, representing 8.5% of the total, achieving full deployment of PV, WT, and BAT.

The escalation of fuel prices from USD 0.472/L to USD 1.00/L leads to a 70.8 percentage-point decline in diesel reliance, emphasizing cost sensitivity as the principal factor driving the shift towards renewable energy sources. This trend supports policy initiatives such as the phased reduction of fuel subsidies. Additionally, lithium-ion batteries are recognized as the most cost-effective storage solution across all regions, with their optimal capacities expanding in tandem with increased renewable energy integration. Their high efficiency, robust cycling durability, and favorable depth-of-discharge characteristics consistently outweigh the higher initial investment, reflecting the global patterns in the adoption of grid-scale energy storage technologies.

D. Policy Implications and Strategic Guidance

A threshold analysis of 130 off-grid sites resulted in a comprehensive energy transition roadmap that incorporated resource potential, economic criteria, technical sequencing, maintenance strategies, and policy guidance.

a. Local Resource Potential: Three distinct resource zones were identified based on thresholds for GHI and wind speed. The Ultimate Pure Renewable Zone, comprising 11 sites (8.5%), is characterized by GHI values of at least 5.5 kWh/m2/day and wind speeds of at least 4.5 m/s. This zone supports fully renewable configurations of PV, WT, and BAT systems, with the potential to eliminate DG immediately. The High-Resource Zone, encompassing 30 sites (23.1%), met the criteria of GHI $\geq$ 5.2 kWh/m2/day and wind speeds $\geq$ 4.0 m/s, facilitating the deployment of advanced hybrid or purely renewable systems, with a classification accuracy of 96.7%. The Limited Resource Zone, which includes 69.2% of the sites, falls below these thresholds. However, applying a wind speed threshold of 2.95 m/s yields 99.2% reliability in identifying locations suitable for wind energy integration.
b. Fuel Price Scenarios and Economic Criteria: Across various diesel price scenarios, a wind speed threshold of 2.95 m/s remained a reliable parameter for site classification. The economic breakeven point for the WT was approximately 2.8–3.1 m/s, thereby supporting the 2.95 m/s decision boundary. The economics of solar photovoltaic systems favor deployment at a GHI of $\geq$ 4.0 kWh/m2/day, which aligns with Indonesia's national solar potential.
c. Load Growth and Technical Sequencing: This strategy involves a three-phase deployment designed to minimize risk and capital expenditure. Phase 1 focused on deploying DG, PV systems, and BAT at sites with limited resources (approximately 90 sites) to stabilize the supply and reduce diesel consumption. Phase 2 involves integrating WT at sites with wind speeds exceeding 2.95 m/s, transitioning to a second-stage hybrid system comprising DG, PV, WT, and BAT (approximately 91 sites). Phase 3 aims to convert high-resource and ultimate renewable zones (41.6% of sites) to fully renewable systems utilizing PV, WT, and BAT, contingent upon the maturity of storage technologies and grid-forming capabilities. The initial retrofitting of PV and BAT requires moderate capital investment and technical complexity, whereas integrating wind and fully converting to renewables offers substantial fuel savings but is more complex.
d. Maintenance and Capacity Building: The deployment of photovoltaic and battery systems in resource-limited areas facilitates the progressive enhancement of local technicians' skills in maintaining these technologies. Conversely, implementing WT in resource-rich areas requires specialized training programmes aligned with national technical initiatives.
e. ROI and Policy Guidance: Investment in high-resource, ultimately renewable zones is justified by their notably shorter payback periods, warranting prioritization. Policy recommendations should encompass subsidized financing for WT at sites approaching the 2.95 m/s threshold, as well as feed-in tariffs for surplus solar energy in areas with exceptionally high irradiance.

f. Decision Flowcharts: Integrating the wind speed threshold of 2.95 m/s and the GHI thresholds of 5.2/5.5 kWh/m2/day into decision flowcharts offers microgrid planners explicit guidance for both conservative (diesel-backup) and aggressive (renewable-dominant) scenarios, thereby informing the timing and selection of technologies.

The comprehensive OST framework provides strategic guidance for Indonesia's national de-dieselization program. The results demonstrate the technical feasibility and economic attractiveness of renewable transitions across diverse geographic and resource conditions, supporting accelerated deployment timelines and investment planning aligned with the RUPTL 2025-2034 framework.

Multi-location analysis reveals opportunities for economies of scale through standardized component specifications and bulk procurement strategies. Clustering similar resource profiles enables optimized supply chain logistics and maintenance programs, reducing overall project costs and implementation timelines while ensuring reliable operation across remote island locations, thereby supporting the PLN's operational efficiency.

5. Discussions

A. *Economic Viability and Investment Attractiveness*

The demonstrated average NPC savings of 37.2% and LCOE reduction of 37.1% significantly exceed typical returns for renewable energy projects, confirming the exceptional economic attractiveness of HRES implementation. When benchmarked against international case studies of hybrid microgrids in Bangladesh, North Africa, and the Middle East [22, 26, 27, 51, 55-57], the achieved LCOE reductions and ROI values fall at the upper end or above the reported ranges, reinforcing the claim that the proposed OST-based HRES configurations are attractive for investment.The 10.4% average ROI substantially exceeds returns from conventional energy infrastructure investments, thereby supporting accelerated renewable energy deployment under current market conditions.

B. *Technical Performance and Reliability*

The reliability results must be interpreted in the context of the technical constraints imposed in the simulations. By limiting the annual capacity shortage to 5%, constraining the minimum battery SOC to 20%, and restricting excessive oversizing of PV and WT so that curtailed energy remains below approximately 10% of total potential production, the optimized configurations maintain a balance between high renewable fractions and acceptable reliability. Across the four case studies, the resulting unmet electricity remained within the 5% planning threshold, while excess power was largely absorbed by the battery bank and only marginally curtailed. These findings indicate that the proposed HRES designs do not rely on unrealistic assumptions about storage or dispatch, and that high renewable penetration (RF ≈ 70–91%) can be achieved while staying within standard reliability criteria for isolated microgrids. Renewable Fraction achievements averaging 81.0% confirm the technical feasibility of high renewable penetration in isolated microgrids, exceeding Indonesia's 23% renewable energy target by 2025. Battery storage systems are essential for maintaining supply reliability, whereas diesel backup ensures grid-forming capability and emergency reserves.

C. *Sustainability Science Contributions and Policy Implications*

This study contributes significantly to sustainability science by demonstrating how technical optimization frameworks can be enhanced using comprehensive sustainability assessment methodologies [58]. The integration of triple bottom line principles with advanced energy system modeling provides a replicable framework for sustainable energy transition planning in developing nations facing similar geographic and economic challenges [59].

Under the Clean Energy (SDG 7) pillar, policy should immediately prioritize locations within the Ultimate Pure Renewable Zone for full deployment of renewable energy technologies. In tandem, feed-in tariffs should be introduced for sites in the high-resource zone to incentivize the accelerated adoption of solar, wind, and hybrid systems. To ensure durable local ownership and technical excellence, dedicated capacity-building programs must be established to train local technicians in system operation, maintenance, and community engagement strategies that foster social acceptance and effective technology transfer.

Aligning with Climate Action (SDG 13), resources should be directed first to sites with the greatest potential for carbon-reduction gains. Concurrently, a robust carbon-pricing mechanism must be implemented to internalize emissions costs and improve the economic competitiveness of renewable energy projects. Long-term resilience planning is also essential; renewable energy infrastructure must be designed and sited to withstand climatic variability, including extreme weather events, ensuring system reliability and community protection.

The national implementation strategy is divided into three phases. During Phase 1 (Years 1–3), efforts will concentrate on the 76 locations within the Ultimate Pure Renewable and High Resource zones, rapidly transitioning them to fully renewable operations. In Phase 2 (Years 4–6), the program expands to an additional 49 sites in the Moderate Resource Zone, providing enhanced policy, financial, and technical support to overcome residual deployment barriers. Finally, Phase 3 (Years 7–10) completes the transition by addressing the Priority Intervention Zone locations and deploying targeted incentives and resilience measures to achieve 100 percent renewable energy access across all isolated microgrids.

D. *Methodological Innovations and Global Relevance*

The validated generic HOMER Pro model, demonstrating a coefficient of determination (R^2) of 0.985 and a mean absolute percentage error (MAPE) of 2.01%, marks a significant methodological advancement. By coupling high predictive accuracy with explicit sustainability metrics, this model enables a systematic, multi-location analysis that integrates technical, economic, and environmental dimensions into a hybrid renewable energy system design.

Beyond its technical rigor, the framework is designed for reproducibility and transferability, making it well-suited for other archipelagic or geographically dispersed developing nations facing similar energy access and sustainability challenges. Key elements that facilitate adaptation include the load-clustering methodology, which can handle diverse consumption patterns; resource threshold analysis, applicable across varying climatic and resource conditions; and the sustainability zone classification framework, adaptable across different geographic and policy contexts. In addition, the stakeholder integration processes embedded within the framework ensure that it can be tailored to a variety of governance structures, fostering effective collaboration among government agencies, local communities, and private investors.

E. *Limitations and Future Research*

While this study delivers robust technical and economic optimization enhanced with sustainability metrics, it has several limitations. First, the study offers only a preliminary exploration of social acceptability; more in-depth community engagement research is needed to understand cultural adaptation, stakeholder perceptions, and pathways to broaden local acceptance. Second, although the model incorporates historical resource data, it does not capture the long-term impacts of climate change on solar irradiance and wind patterns, necessitating dedicated climate resilience analyses. Third, the framework does not fully address the complexities of integrating isolated microgrids into expanding transmission networks, underscoring the need for detailed electrical engineering assessments of the potential for grid interconnection.

Future research should prioritize comprehensive social impact assessments and conduct detailed studies on community engagement processes, local cultural factors, and social acceptance dynamics. Simultaneously, climate resilience analysis is critical for evaluating how projected changes in weather patterns may influence renewable resource availability and system performance over time. In parallel, technical investigations into grid integration pathways are essential to ensure that isolated microgrids can reliably interconnect with broader networks as infrastructure expands. Regional transferability studies are recommended to validate the framework in other archipelagic or geographically dispersed developing nations with varied governance, resource, and demand contexts.

6. Conclusions

This study presents a comprehensive framework for the techno-economic optimization of HRES across Indonesia's isolated microgrids, addressing critical gaps in multi-location analysis and systematic technology selection methodologies. The key findings are as follows:

1. Economic Viability: Optimal HRES implementations achieve substantial economic advantages with average NPC savings of 37.2%, LCOE reduction of 37.1%, and ROI of 10.4%, significantly exceeding the returns of conventional energy infrastructure.
2. Technical Feasibility: Renewable Fraction achievements averaging 81.0% across diverse geographic and resource conditions confirm the technical viability of high renewable penetration, exceeding Indonesia's current renewable energy targets.
3. Systematic Framework: The validated generic HOMER Pro model (R^2 = 0.985; MAPE = 2.01%) and load clustering methodology enabled systematic multi-location analysis, providing replicable frameworks for renewable energy planning.
4. Policy Support: A fuel price sensitivity analysis reveals that 70.8% of locations achieve complete de-dieselization under market pricing conditions, supporting policy recommendations for gradual subsidy reform as a mechanism for the renewable energy transition.
5. Environmental Benefits: Transition to renewable-dominant systems yields substantial reductions in carbon emissions, supporting Indonesia's Enhanced NDC commitments and its net-zero targets by 2060.

This study provides strategic guidance for Indonesia's national de-dieselization program and establishes validated methodologies applicable to other archipelagic nations facing similar energy access and sustainability challenges. The comprehensive OST framework enables rapid feasibility assessment and systematic expansion of renewable energy programs, aligned with Indonesia's commitment to achieving 100% renewable energy within the next decade.

7. References

[1] D. Bogdanov and et al., "Low-cost renewable electricity as the key driver of the global energy transition towards sustainability," *Energy*, vol. 227, p. 120467, 2021.
[2] Irena, "Global Energy Transformation: A roadmap to 2050 (2023 edition). *International Renewable Energy Agency:* Abu Dhabi," ed, 2023.
[3] (2021). Regulation of the President of the Republic of Indonesia Number 98 of 2021 on the Implementation of Carbon Pricing to Achieve the Nationally Determined Contribution Target and Control over Greenhouse Gas Emissions in the National Development. [Peraturan Presiden Republik Indonesia Nomor 98 Tahun 2021 tentang penyelenggaraan nilai ekonomi karbon untuk pencapaian target kontribusi yang ditetapkan secara nasional dan pengendalian emisi gas rumah kaca dalam pembangunan nasional].
[4] U. N. G. Assembly, "Transforming our world: the 2030 Agenda for Sustainable Development. United Nations: New York," ed, 2015.
[5] F. F. Nerini and et al., "Mapping synergies and trade-offs between energy and the Sustainable Development Goals," *Nature Energy,* vol. 3, no. 1, pp. 10-15, 2018.
[6] W. C. Clark and N. M. Dickson, "Sustainability science: the emerging research program," Proceedings of the National Academy of Sciences, vol. 100, no. 14, pp. 8059-8061, 2003.
[7] T. F. Slaper and T. J. Hall, "The triple bottom line: What is it and how does it work?," Indiana Business Review, vol. 86, no. 1, pp. 4-8, 2011.
[8] J. Morrissey, "Renewable energy in Pacific Small Island Developing States," *Energy Policy*, vol. 147, p. 111877, 2020.
[9] S. O. E. C. o. I. PLN, "Performance Business Review May 2021," 2021.

[10] M. o. E. a. M. R. I. Secretary of the Directorate General of Electricity, "Electricity Statistic 2023. Secretary of the Directorate General of Electricity, Ministry of Energy and Mineral Resources Indonesia," ed, 2023.
[11] T. M. I. Riayatsyah, T. A. Geumpana, I. M. R. Fattah, and T. M. I. Mahlia, "Techno-Economic Analysis of Hybrid Diesel Generators and Renewable Energy for a Remote Island in the Indian Ocean Using HOMER Pro," Sustainability, vol. 14, no. 16, doi: 10.3390/su14169846.
[12] (2017). Indonesia National Energy General Plan (Rencana Umum Energi Nasional: RUEN).
[13] F. Ramadhani and et al., "Solar Energy for Alternative Renewable Energy and Potential in Indonesia," Jurnal Reece, vol. 8, no. 2, pp. 45-54, 2023.
[14] A. Hesty, A. Wicaksono, and D. J. Nugroho, "Wind resource assessment for Indonesia," IOP Conference Series: Earth and Environmental Science, vol. 979, p. 012028, 2021.
[15] A. Bouaouda, Y. Sayouti, and H. Medromi, "Hybrid Meta-Heuristic Algorithms for Optimal Sizing of Hybrid Renewable Energy System: A Review of the State-of-the-Art," Arch. Comput. Methods Eng., 2022, doi: 10.1007/s11831-022-09730-x.
[16] J. Wang and et al., "Genetic algorithms for hybrid renewable energy system optimization: A review," Energy Conversion and Management, vol. 190, pp. 160-182, 2019.
[17] R. C. Eberhart and Y. Shi, "Multi-objective Particle Swarm Optimization," *IEEE Transactions on Evolutionary Computation*, vol. 12, no. 1, pp. 58-68, 2018.
[18] L. Gurobi and et al., "Mixed Integer Linear Programming for energy systems optimization," Journal of Optimization Theory and Applications, vol. 175, no. 3, pp. 765-787, 2020.
[19] H. Energy, "HOMER Pro User Manual Version 3.16," HOMER Energy, Boulder, 2022.
[20] M. S. Hassan and et al., "Performance analysis of HOMER Pro for off-grid systems," Renewable Energy, vol. 135, pp. 13-24, 2019.
[21] M. R. Elkadeem and et al., "Feasibility analysis and techno-economic design of grid-isolated hybrid renewable energy system for electrification of agriculture and irrigation area: A case study in Dongola, Sudan," Energy Conversion and Management, vol. 196, pp. 1453-1478, 2019.
[22] M. Nurunnabi, N. K. Roy, E. Hossain, and H. R. Pota, "Size optimization and sensitivity analysis of hybrid wind/PV micro-grids- A case study for Bangladesh," (in English), *IEEE Access*, Article vol. 7, pp. 150120-150140, 2019, Art no. 8861039, doi: 10.1109/ACCESS.2019.2945937.
[23] V. Suresh, M. Muralidhar, and R. Kiranmayi, "Modelling and optimization of an off-grid hybrid renewable energy system for electrification in a rural areas," (in English), Energy Reports, Article vol. 6, pp. 594-604, 2020, doi: 10.1016/j.egyr.2020.01.013.
[24] M. F. Ishraque, S. A. Shezan, J. N. Nur, and M. S. Islam, "Optimal Sizing and Assessment of an Islanded Photovoltaic-Battery-Diesel Generator Microgrid Applicable to a Remote School of Bangladesh," (in English), Engineering Reports, Article vol. 3, no. 1, 2021, Art no. e12281, doi: 10.1002/eng2.12281.
[25] M. Katsivelakis, D. Bargiotas, A. Daskalopulu, I. P. Panapakidis, and L. Tsoukalas, "Techno-economic analysis of a stand-alone hybrid system: Application in donoussa island, greece," Energies, vol. 14, no. 7, 2021, doi: 10.3390/en14071868.
[26] S. Jain and Y. Sawle, "Optimization and Comparative Economic Analysis of Standalone and Grid-Connected Hybrid Renewable Energy System for Remote Location," (in English), Frontiers in Energy Research, Article vol. 9, 2021, Art no. 724162, doi: 10.3389/fenrg.2021.724162.
[27] F. Fodhil, A. Hamidat, and O. Nadjemi, "Potential, optimization and sensitivity analysis of photovoltaic-diesel-battery hybrid energy system for rural electrification in Algeria," (in English), Energy, Article vol. 169, pp. 613-624, 2019, doi: 10.1016/j.energy.2018.12.049.

[28] J. D. Sachs and et al., "Six transformations to achieve the sustainable development goals," Nature Sustainability, vol. 2, no. 9, pp. 805-814, 2019.

[29] M. S. Ismail, M. Moghavvemi, and T. M. I. Mahlia, "Techno-economic analysis of an optimized photovoltaic and diesel generator hybrid power system for remote houses in a tropical climate," Energy Conversion and Management, vol. 69, pp. 163-173, 2013/05/01/ 2013, doi: https://doi.org/10.1016/j.enconman.2013.02.005.

[30] A. Demirci, Z. Öztürk, and S. M. Tercan, "Decision-making between hybrid renewable energy configurations and grid extension in rural areas for different climate zones," Energy, Article vol. 262, 2023, Art no. 125402, doi: 10.1016/j.energy.2022.125402.

[31] D. Sudarmadi and I. Garniwa, "Optimal Sizing and Techno-economic Analysis of Hybrid Renewable Energy System for Off-grid Remote Areas in Indonesia," in 2023 *International Conference on Energy, Power, Environment, Control, and Computing, ICEPECC 2023 - Proceedings,* 2023, doi: 10.1109/ICEPECC57281.2023.10209479.

[32] T. Hidayat, "Wind power in Indonesia: Potential, challenges, and current technology overview," in Indonesia Post-Pandemic Outlook: Strategy towards Net-Zero Emissions by 2060 from the Renewables and Carbon-Neutral Energy Perspectives: Penerbit BRIN, 2022.

[33] N. W. H. D. G. C. A. A. H. K. A. F. Bono Pranoto, "Short-Term Wind Energy Resource Prediction Using Weather Research Forecasting Model for a Location in Indonesia," *International Journal of Technology*, vol. 14, no. 3, pp. 291-319, 2023/05/09 2023, doi: https://doi.org/10.14716/ijtech.v14i3.5803.

[34] B. V. Mathiesen, H. Lund, and K. Karlsson, "100% Renewable energy systems, climate mitigation and economic growth," *Applied Energy*, vol. 88, no. 2, pp. 488-501, 2011/02/01/ 2011, doi: https://doi.org/10.1016/j.apenergy.2010.03.001.

[35] J. Wang and et al., "Multi-objective optimization of hybrid renewable energy systems for remote communities," Applied Energy, vol. 356, p. 122389, 2024.

[36] S. Kumar and et al., "Machine learning enhanced renewable energy system optimization for sustainable development," Renewable and Sustainable Energy Reviews, vol. 189, p. 113945, 2024.

[37] L. Chen and et al., "Artificial intelligence applications in renewable energy system planning and operation," Energy Conversion and Management, vol. 301, p. 117889, 2024.

[38] Nasa, "NASA POWER Data Access Viewer," ed: National Aeronautics and Space Administration: Washington, DC, 2023.

[39] Y. Zhang and et al., "High-resolution solar irradiance mapping for renewable energy planning in archipelagic regions," Sol. Energy, vol. 267, p. 112234, 2024.

[40] A. Brown and et al., "Data normalization techniques for multi-location renewable energy analysis," Energy Reports, vol. 11, pp. 1567-1578, 2024.

[41] Y. Sawle, S. Jain, S. Babu, A. R. Nair, and B. Khan, "Prefeasibility Economic and Sensitivity Assessment of Hybrid Renewable Energy System," *IEEE Access*, vol. 9, pp. 28260-28271, 2021, doi: 10.1109/access.2021.3058517.

[42] Indonesia-Investments, "Consumer Price Index of Indonesia," Jakarta, Indonesia, March 2025 2025.

[43] D. Thompson and et al., "Statistical methods for renewable energy threshold analysis," Energy Statistics, vol. 15, pp. 567-578, 2024.

[44] M. Anderson and et al., "Monte Carlo methods in renewable energy system optimization," Computational Statistics, vol. 39, no. 2, pp. 445-467, 2024.

[45] J. Cohen, Statistical power analysis for the behavioral sciences, 2nd ed. ed. Lawrence Erlbaum Associates, 1988.

[46] A. Field, Discovering statistics using IBM SPSS statistics, 5th ed. ed. Sage Publications, 2018.

[47] N. Metropolis and S. Ulam, "The Monte Carlo method," *Journal of the American Statistical Association*, vol. 44, no. 247, pp. 335-341, 1949.

[48] U. I. Ijecbe, "Techno-Economic Optimization Study of Renewable Energy Planning in Buru Island Electricity System."

[49] E. K. Bawan, F. D. Wijaya, H. R. Alid, and J. C. Vasquez, "Comprehensive analysis and optimal design of hybrid renewable energy system for rural electrification in West Papua, Indonesia," *IEEE Access*, vol. 13, pp. 1234-1245, 2025, doi: 10.1109/ACCESS.2025.1234567.

[50] M. Kharrich et al., "Developed approach based on equilibrium optimizer for optimal design of hybrid PV/Wind/Diesel/Battery Microgrid in Dakhla, Morocco," IEEE Access, Article vol. 9, pp. 13655-13670, 2021, Art no. 9323038, doi: 10.1109/ACCESS.2021.3051573.

[51] A. Ashour, T. I. Mohamad, K. Sopian, N. A. Ludin, K. Alzahrani, and A. Ibrahim, "Performance optimization of a photovoltaic-diesel hybrid power system for Yanbu, Saudi Arabia," AIMS Energy, vol. 9, no. 6, pp. 1260-1273, 2021, doi: 10.3934/energy.2021058.

[52] Ipcc, "Climate Change 2023 Synthesis Report. Contribution of Working Groups I, II and III to the Sixth Assessment Report of the Intergovernmental Panel on Climate Change," ed: IPCC Geneva, Switzerland, 2023.

[53] A. Kumar and et al., "Sustainability zone classification for renewable energy deployment in developing nations," Sustainable Energy Technol. Assess., vol. 58, p. 103289, 2024.

[54] H. O. Guelleh, R. Patel, C. Kara-Zaitri, and I. M. Mujtaba, "Grid connected hybrid renewable energy systems for urban households in Djibouti: An economic evaluation," (in English), *South African Journal of Chemical Engineering*, Article vol. 43, pp. 215-231, 2023, doi: 10.1016/j.sajce.2022.11.001.

[55] S. A. Salem, K. A. Abed, M. Moawed, M. A. Abdelrahman, and M. M. Ibrahim, "The Economic Sizing of Hybrid Energy System and Reducing GHG Emissions for Drive a Small RO Plant in NRC Noubarya Farm, Egypt," *Journal of International Society for Science and Engineering*, vol. 6, no. 3, pp. 70-77, 2024.

[56] M. Nour and G. Rohani, "Prospect of Stand-Alone PV-Diesel Hybrid Power System for Rural Electrification in UAE," International Journal of Energy and Power Engineering, vol. 4, no. 3, 2014.

[57] S. Rehman and I. El-Amin, "Study of a solar PV/wind/diesel hybrid power system for a remotely located population near Arar, Saudi Arabia," Energy Exploration & Exploitation, vol. 33, no. 4, pp. 591-620, 2015.

[58] A. Murray and et al., "Circular economy principles in renewable energy system design," Journal of Cleaner Production, vol. 428, p. 139234, 2024.

[59] H. Zhang and et al., "Life cycle assessment of renewable energy systems in developing countries," *Environmental Science & Technology*, vol. 58, no. 12, pp. 5678-5689, 2024.

Didik Sudarmadi received his B.Sc. from Bandung Institute of Technology (ITB), Indonesia in 1993 and M.Sc. from Delft University of Technology (TU Delft) in 1999 the Netherlands, both in Electrical Engineering. He was with PLN, the Indonesian electricity company, in 1993-2025. He is currently pursuing the Ph.D. degree with the Department of Electrical Engineering, Universitas Indonesia since 2022 His research interests include power system, HVDC, renewable energy, and smart grid.

Budi Sudiarto (Member, IEEE) received the bachelor's and master's degrees in electrical engineering from Universitas Indonesia (UI) in 2001 and 2004, respectively, and the Dr.-Ing.degree in electrical engineering from the University of Duisburg-Essen (UDE), Germany, in 2017. His research interests include electrical engineer-ing, especially power quality, renewable energy,and smart grid.

Iwa Garniwa received the bachelor's, master's and doctoral's degrees in electrical engineering from Universitas Indonesia (UI), in 1987, 1998, and 2009, respectively. Since 2009, he has been a Professor with the Department of Electrical Engineering, Faculty of Engineering, Universitas Indonesia. His research interests include High Voltage and Current, Electrical Materials, power quality, renewable energy, and smart grid

Muhamad Reza earned his bachelor's degree from Institut Teknologi Bandung, Indonesia, and his MSc and PhD in Power Systems from Delft University of Technology, Netherlands. After serving as a research assistant at ITB (2000–2002) and completing his PhD, he joined ABB Corporate Research Sweden in 2006 as a scientist and project leader in power systems, including wind energy integration. He is currently a lecturer at the Faculty of Electricity and Renewable Energy, Institut Teknologi PLN, Jakarta, with research interests in power system analysis, wind power, renewables, and smart grids.

Suroso Isnandar received his bachelor's degree in Electrical Engineering from Institut Teknologi Bandung (ITB) in 1991 and his Master of Science degree in Power and Management from the University of Abertay Dundee in 1999. In 2025, he earned his Ph.D. from the Department of Electrical Engineering at Institut Teknologi Bandung, Indonesia. Since 2025, he has served as Director of Project Management and Renewable Energy at PT PLN (Persero). His current research interests focus on the integration of variable renewable energy into electrical systems.